Deficiency in Bhlhe40 impairs resistance to *H. polygyrus bakeri* and reveals novel Csf2rb-dependent regulation of anti-helminth immunity

Nicholas N. Jarjour[1], Tara R. Bradstreet[1], Elizabeth A. Schwarzkopf[1], Melissa E. Cook[1], Chin-Wen Lai[1], Stanley Ching-Cheng Huang[1,4], Reshma Taneja[2], Thaddeus S. Stappenbeck[1], Steven J. Van Dyken[1], Joseph F. Urban, Jr.[3], Brian T. Edelson[1,5]*

[1]Department of Pathology and Immunology, Washington University School of Medicine, St. Louis, MO 63110. USA

[2]Department of Physiology, Yong Loo Lin School of Medicine, National University of Singapore, Singapore 117597. Singapore

[3]United States Department of Agriculture (USDA), Agricultural Research Service, Beltsville Human Nutrition Research Center, Diet, Genomics, and Immunology Laboratory, Beltsville, MD 20705. USA

[4]Present address: Department of Pathology, Case Western Reserve University School of Medicine, Cleveland, OH 44106. USA

[5]Lead contact

*Correspondence: bedelson@path.wustl.edu

Keywords

Helminth, Bhlhe40, IL-5, GM-CSF, common beta chain, type 2 immunity, T_H2 cell, myeloid, $CD4^+$ T cell, innate immunity

Summary

The type 2 cytokine IL-5 is part of the common beta chain (β_C, Csf2rb) cytokine family and, along with GM-CSF, requires the β_C chain to initiate signaling. The known functions of these two cytokines are largely divergent. Although the helminth *Heligmosomoides polygyrus bakeri* (*H. polygyrus*) elicits IL-5, protective immunity is not dependent on this cytokine. Whether this is due to compensatory mechanisms is unclear. The transcription factor Bhlhe40 has been shown to control GM-CSF production and is proposed to be a novel regulator of T helper type 2 cells. We have found that Bhlhe40 is required in T cells for a protective memory response to secondary *H. polygyrus* infection. *H. polygyrus* rechallenge elicited dramatic Bhlhe40-dependent changes in gene and cytokine expression by lamina propria $CD4^+$ T cells including induction of GM-CSF and maximal production of type 2 cytokines including IL-5. β_C chain-deficient, but not GM-CSF-deficient, mice rechallenged with *H. polygyrus* had severely impaired protective immunity. Our results demonstrate that Bhlhe40 is an essential regulator of $CD4^+$ T cell immunity during helminth infection and reveal a critical role for redundant β_C chain-dependent cytokines during anti-helminth immunity.

Introduction

Helminthic worms are parasites of eukaryotic organisms which manipulate the immune system to establish chronic infections in diverse sites, often resulting in significant tissue damage (Allen and Sutherland, 2014; Maizels et al., 2018; Patel et al., 2009; Sorobetea et al., 2018). A stereotypical helminth infection results in production of alarmins including IL-25, IL-33, and thymic stromal lymphopoietin (TSLP), which in turn stimulate the development of type 2 immunity characterized by production of IL-4, IL-5, and IL-13 (Allen and Sutherland, 2014; Maizels et al., 2018; Sorobetea et al., 2018). The helminth *Heligmosomoides polygyrus bakeri* (hereafter *H. polygyrus*) is a natural pathogen of mice and has been frequently employed as a

model helminth infection (Camberis et al., 2003; Maizels et al., 2018; Patel et al., 2009; Sorobetea et al., 2018). Several cytokines contribute to protective immunity against *H. polygyrus*, including IL-4 and IL-25, while IL-5, IL-33, and TSLP are considered dispensable for control of this infection (Massacand et al., 2009; Pei et al., 2016; Urban et al., 1991; Zaiss et al., 2013).

However, in many instances of type 2 immunity, IL-5 plays a crucial role (Bagnasco et al., 2017; Roufosse, 2018), including in some helminth infections (Allen and Sutherland, 2014; Maizels et al., 2004; Sorobetea et al., 2018). Controversy previously existed as to whether IL-5 was protective against helminths, but it is now appreciated that deficiency in IL-5 only affects immunity to select parasites and sometimes in a life cycle stage-dependent manner (Allen and Sutherland, 2014; Maizels et al., 2004). IL-5 binds to the unique IL-5Rα chain paired with the common beta (β_C) chain, which is shared with the receptors for GM-CSF and IL-3 (Dougan et al., 2019; Robb et al., 1995). This raises the possibility that redundancy within this cytokine family could render individual members dispensable during helminth infection. While IL-3 signaling is maintained in mice in the absence of the β_C chain (*Csf2rb*) through a unique beta chain (β_{IL3}, *Csf2rb2*), GM-CSF and IL-5 signaling is abrogated in *Csf2rb*$^{-/-}$ mice (Dougan et al., 2019; Robb et al., 1995). Despite absolute dependence on this shared receptor chain, which is largely responsible for downstream signaling (Dougan et al., 2019), known roles for IL-5 and GM-CSF are divergent. GM-CSF has been proposed to be a central regulator of inflammation driven by T_H1 and T_H17 cells and affects both autoimmunity and infection (Becher et al., 2016; Croxford et al., 2015; Deepe et al., 1999; Gonzalez-Juarrero et al., 2005; Hirata et al., 2010; LeVine et al., 1999; Mandujano et al., 1995; Paine et al., 2000; Zhan et al., 1998). GM-CSF also contributes to pathological T_H2 responses to allergens (Cates et al., 2004; Sheih et al., 2017; Yamashita et al., 2002). However, little is known regarding GM-CSF during type 2 infections,

though it is thought to be dispensable during infection with the helminth *Nippostrongylus brasiliensis* (Shim et al., 2012).

The transcription factor Bhlhe40 functions in B cells, NKT cells, T cells, and tissue-resident macrophages (Camponeschi et al., 2018; Huynh et al., 2018; Jarjour et al., 2019; Kanda et al., 2016; Kreslavsky et al., 2017; Lin et al., 2016; Lin et al., 2014; Martínez-Llordella et al., 2013; Seimiya et al., 2004; Yu et al., 2018). We and others have described a crucial role for Bhlhe40 as a modulator of T_H1 and T_H17 cell cytokine production in infection and autoimmunity, particularly by controlling GM-CSF and IL-10 production (Huynh et al., 2018; Lin et al., 2016; Lin et al., 2014; Martínez-Llordella et al., 2013; Yasuda et al., 2019; Yu et al., 2018). Recent studies of *in vitro*-polarized T_H2 cells (Henriksson et al., 2019) and house dust mite (HDM)-elicited airway T_H2 cells (Tibbit et al., 2019) have identified Bhlhe40 as a potential regulator of this cell type *in vivo*. We have also recently described a role for Bhlhe40 in large peritoneal macrophages (LPMs) during type 2 immunity (Jarjour et al., 2019). Taken together, these data suggest that Bhlhe40 may regulate type 2 infections, possibly by controlling cytokine production from T cells or via a myeloid cell-intrinsic role.

Herein, we have found that Bhlhe40 and the β_C chain are essential to protective memory to secondary *H. polygyrus* infection. *Bhlhe40*$^{-/-}$ mice exhibited severe defects during rechallenge infection with *H. polygyrus* and altered intestinal pathology, which were recapitulated in *Cd4-Cre*$^{+}$ *Bhlhe40*$^{fl/fl}$, but not *LysM-Cre*$^{+}$ *Bhlhe40*$^{fl/fl}$ mice. We defined a helminth-induced gene signature in lamina propria CD4^{+} T cells, which was disrupted in the absence of Bhlhe40. Infection with *H. polygyrus* elicited Bhlhe40-dependent production of GM-CSF from CD4^{+} T cells, and Bhlhe40-deficient CD4^{+} T cells also exhibited reduced production of IL-5. Secondary infection of *Csf2rb*$^{-/-}$, but not *Csf2*$^{-/-}$, mice resulted in severely impaired protective immunity and altered intestinal pathology. Overall, Bhlhe40 serves as a pivotal regulator of the CD4^{+} T cell transcriptional response to helminth infection, in part by modulating GM-CSF and IL-5

production, and reveals redundant roles for these cytokines not observed during deficiency of either factor alone.

Results

Bhlhe40 is required for control of *H. polygyrus* rechallenge

Primary oral challenge of C57BL/6 mice with *H. polygyrus* results in chronic infection, but rechallenge evokes a protective recall response which limits infection (Filbey et al., 2014). To assess whether Bhlhe40 was required for immunity to *H. polygyrus*, we challenged C57BL/6 *Bhlhe40*$^{+/+}$ and *Bhlhe40*$^{-/-}$ mice with infective *H. polygyrus* larvae (L3), cured them by treatment with pyrantel pamoate, and rechallenged them with infective L3. While *Bhlhe40*$^{+/+}$ and *Bhlhe40*$^{-/-}$ mice exhibited similar parasite fecal egg burdens during primary infection, *Bhlhe40*$^{-/-}$ mice had a much higher egg burden during secondary infection as compared to *Bhlhe40*$^{+/+}$ mice **(Figure 1A)**. While there was a trend towards increased adult worm burden in *Bhlhe40*$^{-/-}$ as compared to *Bhlhe40*$^{+/+}$ mice after rechallenge **(Figure 1B)**, this did not reach statistical significance, indicating that their increased egg burden was primarily due to increased worm fecundity. *H. polygyrus*-rechallenged *Bhlhe40*$^{+/+}$ and *Bhlhe40*$^{-/-}$ mice had dramatically different pathology. Type 2 granulomas can form around developing parasites and have been correlated with protective immunity (Filbey et al., 2014). Small intestines from *Bhlhe40*$^{+/+}$ mice exhibited many granulomas, while those from *Bhlhe40*$^{-/-}$ mice resembled healthy tissue **(Figure 1C and 1D)**. Histological analysis and immunostaining showed reduced immune infiltration and damage to the smooth muscle layer in *H. polygyrus*-rechallenged *Bhlhe40*$^{-/-}$ as compared to *Bhlhe40*$^{+/+}$ mice **(Figure 1E and 1F)**.

When we explored the cellular composition of the small intestine lamina propria (SILP) following *H. polygyrus* rechallenge of *Bhlhe40*$^{+/+}$ mice by flow cytometry, we found both

CD45$^+$CD64$^+$F4/80$^+$MHC-II$^+$Ly6C$^-$ resident macrophages (Bain et al., 2014; Scott et al., 2017) and another CD45$^+$F4/80$^+$CD64$^+$MHC-II^{lo}Ly6C^{lo} autofluorescent population, which we termed granuloma-associated monocytes/macrophages (GMMs) **(Figure 1G and 1H)**. This latter population may correspond to previously described clodronate-sensitive alternatively activated macrophages seen by immunostaining during *H. polygyrus* infection (Anthony et al., 2006). SILP CD45$^+$F4/80$^+$CD64$^-$CD11b$^+$SSC-A^{hi} eosinophils were also significantly increased after secondary *H. polygyrus* infection **(Figures 1G, 1H, and S1A)**. However, GMMs and eosinophils were greatly reduced in *H. polygyrus*-rechallenged *Bhlhe40*$^{-/-}$ as compared to *Bhlhe40*$^{+/+}$ mice, in contrast to SILP CD3$^+$ T cells **(Figure 1G, 1H, and S1B)**. When we assessed accumulation of LPMs and peritoneal eosinophils, we found severe reductions in both populations in *H. polygyrus*-rechallenged *Bhlhe40*$^{-/-}$ as compared to *Bhlhe40*$^{+/+}$ mice, as well as impaired LPM polarization as assessed by RELMα staining **(Figure S1B-S1G)**. In contrast, serum *H. polygyrus*-specific IgG1 titers were not affected by loss of Bhlhe40 **(Figure 1I)**. These data indicated impaired responses by multiple myeloid cell lineages to *H. polygyrus* rechallenge in *Bhlhe40*$^{-/-}$ mice.

Bhlhe40 is required in T cells for a normal immune response to *H. polygyrus*

We next employed *Cd4-Cre*$^+$ *Bhlhe40*$^{fl/fl}$ and *LysM-Cre*$^+$ *Bhlhe40*$^{fl/fl}$ mice to address whether loss of Bhlhe40 specifically in T cells or myeloid cells recapitulated the phenotype of *Bhlhe40*$^{-/-}$ mice during secondary *H. polygyrus* infection. *Cd4-Cre*$^+$ *Bhlhe40*$^{fl/fl}$ mice were severely impaired in controlling *H. polygyrus* rechallenge and lacked intestinal granulomas as compared to *Cd4-Cre*$^-$ *Bhlhe40*$^{fl/fl}$ mice **(Figure 2A and 2B)**. When we assessed the response of myeloid cells to secondary infection, we found that loss of Bhlhe40 selectively in T cells was sufficient to perturb both the SILP and peritoneal responses **(Figures 2C and S1H-S1J)**. In contrast, *LysM-Cre*$^+$ *Bhlhe40*$^{fl/fl}$ mice were able to control infection and formed intestinal granulomas comparably to

LysM-Cre^{-} *Bhlhe40*$^{fl/fl}$ mice **(Figure 2D and 2E)**. Therefore, Bhlhe40 expression was required in T cells to control secondary *H. polygyrus* infection, but was dispensable in LysM-expressing myeloid cells.

Bhlhe40 is required for a normal CD4^{+} T cell transcriptional response to *H. polygyrus*

We next asked whether loss of Bhlhe40 dysregulated CD4^{+} T cell gene expression in response to *H. polygyrus* rechallenge. To address this, we sorted CD4^{+} T cells from the SILP of naïve and rechallenged *Bhlhe40*$^{+/+}$ and *Bhlhe40*$^{-/-}$ mice for gene expression microarrays. By comparing CD4^{+} T cells from naïve and *H. polygyrus*-rechallenged *Bhlhe40*$^{+/+}$ mice, we defined a helminth-induced signature which included transcripts for cytokines (including *Areg*, *Il3*, *Il4*, *Il5*, *Il6*, *Il13*, *Csf1*, *Csf2, Lif*, *Tnf*, *Tnfsf11*), cytokine receptors (including *Il1rl1*, *Il1r2*, *Il17rb*), and transcription factors (including *Atf3*, *Bhlhe40*, *Gata3*, *Nfil3*, *Pparg*, *Rbpj*, *Vdr*, and *Zeb2*) **(Figures 3A and S2A)**. When we assessed Bhlhe40-dependent genes after *H. polygyrus* rechallenge, we found that a significant majority were part of the helminth-induced signature and that Bhlhe40-dependent genes were distinct in CD4^{+} T cells from naïve and *H. polygyrus*-rechallenged mice **(Figures 3B, 3C, S2B, and S2C)**. When we used gene set enrichment analysis (GSEA) to look for Bhlhe40-dependent gene modules, we noted that two of the most enriched sets in *Bhlhe40*$^{+/+}$ as compared to *Bhlhe40*$^{-/-}$ CD4^{+} T cells after *H. polygyrus* rechallenge were “growth factor activity” and “cytokine activity,” reflecting altered expression of cytokine genes including *Areg*, *Il5*, *Il6*, *Il13*, *Csf1*, *Csf2*, and *Lif*, but not *Il3*, *Il4*, or *Tnf* **(Figure 3D and 3E)**. Furthermore, when we assessed differential expression of the lineage-specifying transcription factors of each T helper cell subset as well as a recently defined set of transcriptional regulators of *in vitro*-polarized T_H2 cells (Henriksson et al., 2019), we observed reduced expression of *Pparg* in *Bhlhe40*$^{-/-}$ as compared to *Bhlhe40*$^{+/+}$ CD4^{+} T cells from *H. polygyrus*-rechallenged mice (2.4-fold reduced), but only subtle changes in other factors including *Gata3* (1.4-fold reduced)

(Figure 3E). *Bhlhe40* expression was markedly induced in mice experiencing secondary infection as compared to naïve mice **(Figure 3E)**. Using *Bhlhe40*^{GFP} bacterial artificial chromosome reporter mice (Lin et al., 2016), we observed a marked increase in SILP GFP^{+} CD4^{+} T cells after *H. polygyrus* rechallenge **(Figure 3F)**. Taken together, these data showed that Bhlhe40 was induced by SILP CD4^{+} T cells in response to *H. polygyrus* rechallenge and was critical for their normal transcriptional program.

Loss of Bhlhe40 impairs T cell cytokine production in response to *H. polygyrus*

Next, we restimulated SILP cells from naïve and rechallenged *Cd4-Cre*$^{-}$ *Bhlhe40*$^{fl/fl}$ and *Cd4-Cre*$^{+}$ *Bhlhe40*$^{fl/fl}$ mice *in vitro* with phorbol 12-myristate 13-acetate (PMA) and ionomycin to assess cytokine production. Rechallenge with *H. polygyrus* induced production of IL-4, IL-5, and IL-13 from *Cd4-Cre*$^{-}$ *Bhlhe40*$^{fl/fl}$ and *Cd4-Cre*$^{+}$ *Bhlhe40*$^{fl/fl}$ CD4^{+} T cells; however, Bhlhe40 was required for normal frequencies of single- and multi-cytokine-producing cells, largely due to reductions in IL-5^{+} and IL-13^{+} CD4^{+} T cells **(Figure 4A-4C)**. Because *Csf2* was upregulated by *H. polygyrus* rechallenge in a Bhlhe40-dependent fashion, we also assessed GM-CSF and found that it was markedly induced by rechallenge (~35% of *Cd4-Cre*$^{-}$ *Bhlhe40*$^{fl/fl}$ CD4^{+} T cells) and that this required Bhlhe40 (~10% of *Cd4-Cre*$^{+}$ *Bhlhe40*$^{fl/fl}$ CD4^{+} T cells) **(Figure 4D and 4E)**. T_H2 cells disseminate widely in mice infected with *H. polygyrus* (Mohrs et al., 2005; Steinfelder et al., 2017). CD4^{+} T cell cytokine responses in the peritoneal cavity and mesenteric lymph nodes from *H. polygyrus*-rechallenged *Cd4-Cre*$^{-}$ *Bhlhe40*$^{fl/fl}$ and *Cd4-Cre*$^{+}$ *Bhlhe40*$^{fl/fl}$ mice were generally consistent with those in the SILP **(Figure S3A and S3B)**. As Bhlhe40 is a known repressor of IL-10 (Huynh et al., 2018; Lin et al., 2016; Lin et al., 2014; Yu et al., 2018), we also assessed IL-10 production from CD4^{+} T cells. Indeed, SILP CD4^{+} T cells lacking Bhlhe40 produced significantly higher levels of IL-10 after *H. polygyrus* rechallenge **(Figure S4A)**. Nevertheless, genetic deletion of IL-10 in *Bhlhe40*$^{-/-}$ *Il10*$^{-/-}$ mice was not sufficient to restore

control of infection or normal intestinal granulomatous pathology **(Figure S4B and S4C)**. These data demonstrated a key role for Bhlhe40 in $CD4^+$ T cell cytokine responses to helminth infection, notably controlling production of the β_C chain family cytokines IL-5 and GM-CSF.

Loss of the β_C chain impairs protective memory to *H. polygyrus*

As protective memory responses to *H. polygyrus* rechallenge are unaffected by IL-5 blockade (Urban et al., 1991), we first asked whether loss of GM-CSF signaling was sufficient to impair control of a secondary infection with *H. polygyrus*. Genetic deletion of GM-CSF (*Csf2*$^{-/-}$ mice) or anti-GM-CSF antibody (αGM-CSF) treatment did not result in severe defects in control of *H. polygyrus* infection as compared to *Csf2*$^{+/+}$ mice or control IgG treatment, respectively **(Figure S4D-S4L)**. As IL-5 and GM-CSF were individually dispensable, we then rechallenged *Csf2rb*$^{+/+}$ and *Csf2rb*$^{-/-}$ mice. Remarkably, *Csf2rb*$^{-/-}$ mice had a severe defect in control of *H. polygyrus* as compared to *Csf2rb*$^{+/+}$ mice **(Figure 4F)**. *Csf2rb*$^{-/-}$ mice did not form intestinal granulomas or develop a normal SILP myeloid cell response to *H. polygyrus* rechallenge as compared to *Csf2rb*$^{+/+}$ mice **(Figure 4G and 4H)**. Furthermore, loss of the β_C chain resulted in defects in peritoneal myeloid cell responses similar to those seen in *Bhlhe40*$^{-/-}$ and *Cd4-Cre*$^+$ *Bhlhe40*$^{fl/fl}$ mice **(Figure S4M-S4O)**. Taken together, these data indicated that β_C chain-dependent cytokines were collectively, but not individually, critical to control of *H. polygyrus* rechallenge.

Discussion

We have demonstrated that protective memory responses against *H. polygyrus* are critically dependent on Bhlhe40 and the β_C chain. Bhlhe40 is specifically required in $CD4^+$ T cells to promote a normal myeloid cell response to *H. polygyrus* by supporting expression of cytokine transcripts as well as other potential regulators of helminth infection, including *Areg*, *Csf2*, *Il5*,

Il13, *Nlrp3*, and *Pparg* (Chen et al., 2017; Chenery et al., 2019; Zaiss et al., 2006). We have also described the $CD4^+$ T cell transcriptome within the SILP during secondary *H. polygyrus* infection. These data provide unique insight into the $CD4^+$ T cell global transcriptional response to helminths at the site of infection. GM-CSF and IL-5 were markedly stimulated by *H. polygyrus* rechallenge and this response was Bhlhe40-dependent. In light of these data, we assessed the importance of the β_C chain during *H. polygyrus* rechallenge and found that it was critically required for protective immunity, despite control of secondary *H. polygyrus* infection during IL-5 blockade (Urban et al., 1991), during GM-CSF blockade, and in *Csf2*$^{-/-}$ mice. These data support redundant roles for Bhlhe40-dependent β_C chain-dependent cytokines in protective immunity to *H. polygyrus*.

When we compared differentially expressed transcripts between *H. polygyrus*-elicited and naive SILP $CD4^+$ T cells, we found a remarkable similarity to the transcriptional profile of HDM-elicited airway T_H2 cells (*Bhlhe40*, *Cd200r1*, *Il6*, *Plac8*, *Igfbp7*) (Tibbit et al., 2019), demonstrating significant conservation of the T_H2 transcriptional program independent of tissue environment and stimulus. When we assessed whether Bhlhe40 was functionally required in T cells during type 2 immunity, we found that SILP $CD4^+$ T cells activated by *H. polygyrus* rechallenge required Bhlhe40 for normal expression of many helminth-induced genes and to control helminth rechallenge. We therefore demonstrate for the first time that Bhlhe40 regulates *in vivo* T_H2 cell responses, consistent with a recent screen for novel regulators of *in vitro*-polarized T_H2 cells that identified Bhlhe40 (Henriksson et al., 2019). Notably, *Pparg* expression was reduced in the absence of Bhlhe40, and as PPARγ is required for normal T_H2 cell responses and protective immunity to *H. polygyrus*, this may indicate that some of the effects of Bhlhe40 deficiency are indirect (Chen et al., 2017; Nobs et al., 2017). Our work and that of others has now established key roles for Bhlhe40 in T_H1, T_H2, and T_H17 cells as a pivotal regulator of GM-CSF, IL-10, and other cytokines (Huynh et al., 2018; Lin et al., 2016; Lin et al.,

2014; Martínez-Llordella et al., 2013; Yasuda et al., 2019; Yu et al., 2018). These data and recent work on c-Maf (Gabrysova et al., 2018) suggest that T cell production of many cytokines may be controlled by multi-lineage transcription factors in addition to lineage-restricted factors. In light of the critical role for Bhlhe40 in multiple $CD4^+$ T cell subsets, clinical targeting of factors regulating Bhlhe40 may possess significant therapeutic potential.

While GM-CSF and IL-5 have long been known to share common signaling through the β_C chain, their described functions are largely distinct, with GM-CSF contributing to T_H1 and T_H17 cell-driven inflammation and IL-5 contributing to type 2 immunity (Bagnasco et al., 2017; Becher et al., 2016; Codarri et al., 2011; Roufosse, 2018). We have demonstrated β_C chain-dependent protective memory to a helminth infection previously shown to be unaffected by IL-5 blockade (Urban et al., 1991) and which we now show to be insensitive to GM-CSF deficiency. It remains to be determined how GM-CSF and IL-5 compensate for each other, whether by direct substitution or via effects on distinct arms of the type 2 response. While redundancy between β_C chain family cytokines is not well described, it is known that these cytokines can regulate eosinophils in a complementary manner (Esnault and Kelly, 2016). Future studies should establish whether GM-CSF and IL-5 are collectively involved in protective immunity to other helminth infections. As β_{IL3} chain-dependent IL-3 signaling is preserved in *Csf2rb*$^{-/-}$ mice (Dougan et al., 2019; Robb et al., 1995), it is also of interest to establish whether additionally blocking IL-3 results in a more severe defect in immunity to *H. polygyrus* than is observed in *Csf2rb*$^{-/-}$ mice. IL-3 regulates basophilia in response to *H. polygyrus* and basophils help control infection with this helminth (Herbst et al., 2012; Schwartz et al., 2014), suggesting that IL-3 is likely important for control of *H. polygyrus* infection.

Our findings reveal novel transcriptional and cytokine regulation of the immune response to helminth infection, elucidating a critical role for Bhlhe40 and unexpected functions of β_C chain-dependent signaling. Our data suggest that the importance of β_C chain family cytokines

may have been underestimated in type 2 diseases because of redundancy. Further studies are needed to elucidate whether compensation between β_C chain family cytokines is a general theme of type 2 immunity and whether combinatorial targeting of these factors could yield improved clinical outcomes in diseases of pathological type 2 immunity.

Acknowledgements

This work was supported by the National Institute of Allergy and Infectious Disease (NIAID) (AI113118 and AI132653) (B.T.E.) and a Burroughs Wellcome Fund Career Award for Medical Scientists (B.T.E.). N.N.J. was supported by grant 5T32AI007163 from the NIAID. S.C.-C.H. was supported by a Case Comprehensive Cancer Center American Cancer Society IRG Award (IRG-16-186-21) and a Cleveland Digestive Diseases Research Core Center Pilot Award (P30DK097948). M.E.C. was supported by the National Science Foundation Graduate Research Fellowship program (DGE-1745038). Research reported in this publication was supported by the Washington University Institute of Clinical and Translational Sciences grant UL1TR002345 from the National Center for Advancing Translational Sciences (NCATS) of the National Institutes of Health (NIH). The content is solely the responsibility of the authors and does not necessarily represent the official view of the NIH. We thank N. Zhang, B. Saunders, and G. Randolph for help with microscopy and technical advice. We thank E. Lantelme, D. Brinja, and A. Mitra for help with fluorescence activated cell-sorting. We thank J. Bando for help with flow cytometry of the gut.

Author Contributions

N.N.J designed, performed, and analyzed experiments and wrote the manuscript. E.A.S., T.R.B., M.E.C., C.-W. L., and S.J.V.D. performed experiments. S.C.-C.H. provided reagents, protocols, and technical expertise. R.T. provided mice. T.S.S., S.J.V.D. and J.F.U. provided

reagents and technical expertise. B.T.E. designed and analyzed experiments, supervised the studies, and wrote the manuscript.

Declaration of Interests

The authors declare no competing interests.

Figure Legends

Figure 1. Bhlhe40 is required for a protective recall response to *H. polygyrus*. (A-C) *H. polygyrus*-infected *Bhlhe40*$^{+/+}$ and *Bhlhe40*$^{-/-}$ mice were analyzed for **(A)** quantitation of *H. polygyrus* eggs/gram feces over time during secondary infection, **(B)** quantitation of adult worms recovered from the intestines of mice experiencing primary or secondary infection, and **(C)** small intestine morphology after secondary infection. Arrows point to granulomas. Scale bar, 1 cm. **(D)** Quantitation of intestinal granulomas. **(E and F)** *H. polygyrus*-rechallenged *Bhlhe40*$^{+/+}$ and *Bhlhe40*$^{-/-}$ mice were analyzed histologically on adjacent sections by **(E)** hematoxylin and eosin staining and **(F)** immunostaining for F4/80, α-SMA, and DAPI performed on swiss rolls of the proximal small intestine (2 representative lesions from each genotype). G, granuloma. M, muscle layers. P, peritoneal space. V, villi. Scale bar, 200 μm. **(G and H)** Naïve and *H. polygyrus*-rechallenged *Bhlhe40*$^{+/+}$ and *Bhlhe40*$^{-/-}$ mice were analyzed by flow cytometry for **(G)** SILP myeloid cells and **(H)** quantitation as in **(G)**. **(I)** Naïve and *H. polygyrus*-rechallenged *Bhlhe40*$^{+/+}$ and *Bhlhe40*$^{-/-}$ mice were analyzed for serum anti-*H. polygyrus* IgG1 titers. Data are pooled from at least 3 independent experiments **(A, B, D, H)** or 2 independent experiments **(I)**. Data in **(C, E-G)** are representative of at least 3 independent experiments. Data are mean ± s.e.m. Significance calculated with an unpaired Student's *t*-test. See also Figure S1.

Figure 2. Bhlhe40 is required in T cells for a normal memory response to *H. polygyrus*. **(A)** *H. polygyrus*-rechallenged *Cd4-Cre*$^{-}$ *Bhlhe40*$^{fl/fl}$ and *Cd4-Cre*$^{+}$ *Bhlhe40*$^{fl/fl}$ mice were analyzed for quantitation of *H. polygyrus* eggs/gram feces over time. **(B)** Naïve and *H. polygyrus*-rechallenged *Cd4-Cre*$^{-}$ *Bhlhe40*$^{fl/fl}$ and *Cd4-Cre*$^{+}$ *Bhlhe40*$^{fl/fl}$ mice were analyzed for quantitation of intestinal granulomas. **(C)** Naïve and *H. polygyrus*-rechallenged *Cd4-Cre*$^{-}$ *Bhlhe40*$^{fl/fl}$ and *Cd4-Cre*$^{+}$ *Bhlhe40*$^{fl/fl}$ mice were analyzed by flow cytometry for quantitation of SILP myeloid cells. **(D)** *H. polygyrus*-rechallenged *LysM-Cre*$^{-}$ *Bhlhe40*$^{fl/fl}$ and *LysM-Cre*$^{+}$ *Bhlhe40*$^{fl/fl}$ mice were analyzed for quantitation of *H. polygyrus* eggs/gram feces over time. **(E)** Naïve and *H. polygyrus*-rechallenged *LysM-Cre*$^{-}$ *Bhlhe40*$^{fl/fl}$ and *LysM-Cre*$^{+}$ *Bhlhe40*$^{fl/fl}$ mice were analyzed for quantitation of intestinal granulomas. Data are pooled from 3 independent experiments **(A-C)** or 2 independent experiments **(D and E)**. Data are mean ± s.e.m. Significance calculated with an unpaired Student's *t*-test. See also Figure S1.

Figure 3. Loss of Bhlhe40 dysregulates the CD4^{+} T cell transcriptional response to *H. polygyrus* rechallenge. (A and B) Gene expression microarray data were analyzed for the 100 most differentially expressed probe sets in SILP CD4^{+} T cells from **(A)** naïve and *H. polygyrus*-rechallenged *Bhlhe40*$^{+/+}$ mice and **(B)** *H. polygyrus*-rechallenged *Bhlhe40*$^{+/+}$ and *Bhlhe40*$^{-/-}$ mice. **(C)** Gene expression microarray data were analyzed for shared and unique Bhlhe40-dependent genes (≥2-fold differentially expressed between SILP CD4^{+} T cells from *H. polygyrus*-rechallenged *Bhlhe40*$^{+/+}$ and *Bhlhe40*$^{-/-}$ mice) with the helminth-induced signature (≥2-fold differentially expressed between SILP CD4^{+} T cells from naïve and *H. polygyrus*-rechallenged *Bhlhe40*$^{+/+}$ mice), depicted as a Venn diagram. **(D)** GSEA of gene expression microarray data for selected C5 gene sets enriched in *Bhlhe40*$^{+/+}$ versus *Bhlhe40*$^{-/-}$ SILP CD4^{+} T cells from *H. polygyrus*-rechallenged mice. NES, normalized enrichment score. FWER, family-wise error rate. **(E)** Gene expression microarray data were analyzed for (left) expression of

cytokines induced by *H. polygyrus* rechallenge and (right) expression of T_H2 and T helper cell lineage-specifying transcription factors in SILP $CD4^+$ T cells from naïve and *H. polygyrus*-rechallenged *Bhlhe40*$^{+/+}$ and *Bhlhe40*$^{-/-}$ mice. TF, transcription factor. **(F)** Flow cytometry of *Bhlhe40*^{GFP} transgene reporter expression in SILP $CD4^+$ T cells from *Bhlhe40*$^{GFP+}$ mice. Microarray data and *Bhlhe40*^{GFP} data are from single experiments. See also Figure S2.

Figure 4. Bhlhe40 is required for normal $CD4^+$ T cell production of β_C chain-dependent cytokines necessary for control of *H. polygyrus* rechallenge. (A-C) Naïve and *H. polygyrus*-rechallenged *Cd4-Cre*$^-$ *Bhlhe40*$^{fl/fl}$ and *Cd4-Cre*$^+$ *Bhlhe40*$^{fl/fl}$ mice were analyzed by flow cytometry for **(A)** IL-4-, IL-5-, and IL-13-producing $CD4^+$ T cells, **(B)** quantitation of the frequency of IL-4^+, IL-5^+, and IL-13^+ $CD4^+$ T cells, and **(C)** quantitation of the frequency of $CD4^+$ T cells producing one or more cytokines after *in vitro* PMA/ionomycin stimulation of SILP cells. **(D and E)** Naïve and *H. polygyrus*-rechallenged *Cd4-Cre*$^-$ *Bhlhe40*$^{fl/fl}$ and *Cd4-Cre*$^+$ *Bhlhe40*$^{fl/fl}$ mice were analyzed by flow cytometry for **(D)** GM-CSF-producing $CD4^+$ T cells and **(E)** quantitation as in **(D)** after *in vitro* PMA/ionomycin stimulation of SILP cells. **(F)** *H. polygyrus*-rechallenged *Csf2rb*$^{+/+}$ and *Csf2rb*$^{-/-}$ mice were analyzed for quantitation of *H. polygyrus* eggs/gram feces over time. **(G)** Naïve and *H. polygyrus*-rechallenged *Csf2rb*$^{+/+}$ and *Csf2rb*$^{-/-}$ mice were analyzed for quantitation of intestinal granulomas. **(H)** Naïve and *H. polygyrus*-rechallenged *Csf2rb*$^{+/+}$ and *Csf2rb*$^{-/-}$ mice were analyzed by flow cytometry for quantitation of SILP myeloid cells. Data are representative of 2 independent experiments **(A and D)** or are pooled from 2 independent experiments **(B, C, E-H)**. Data are mean ± s.e.m. Significance calculated with an unpaired Student's *t*-test. See also Figures S3 and S4.

Figure S1. Loss of Bhlhe40 dysregulates myeloid cell responses to *H. polygyrus* rechallenge. Related to Figures 1 and 2. (A and B) Naïve and *H. polygyrus*-rechallenged *Bhlhe40*$^{+/+}$ and *Bhlhe40*$^{-/-}$ mice were analyzed by flow cytometry for **(A)** SILP eosinophils and **(B)** quantitation of SILP CD3^{+} T cells. **(C and D)** Naïve and *H. polygyrus*-rechallenged *Bhlhe40*$^{+/+}$ and *Bhlhe40*$^{-/-}$ mice were analyzed by flow cytometry for **(C)** peritoneal eosinophils and **(D)** quantitation as in **(C)**. **(E-G)** Naïve and *H. polygyrus*-rechallenged *Bhlhe40*$^{+/+}$ and *Bhlhe40*$^{-/-}$ mice were analyzed by flow cytometry for **(E)** LPMs, **(F)** quantitation as in **(E)**, and **(G)** quantitation of the frequency of RELMα^{+} LPMs. **(H-J)** Naïve and *H. polygyrus*-rechallenged *Cd4-Cre*$^{-}$ *Bhlhe40*$^{fl/fl}$ and *Cd4-Cre*$^{+}$ *Bhlhe40*$^{fl/fl}$ mice were analyzed by flow cytometry for quantitation of **(H)** peritoneal eosinophils, **(I)** LPMs, and **(J)** the frequency of RELMα^{+} LPMs. Data are representative of at least three independent experiments **(A, C, E)** or are pooled from at least 3 independent experiments **(B, D, F-J)**. Data are mean ± s.e.m. Significance calculated with an unpaired Student's *t*-test.

Figure S2. Bhlhe40 regulates distinct gene sets in CD4^{+} T cells from naïve and *H. polygyrus*-rechallenged mice. Related to Figure 3. (A) Gene expression microarray data were analyzed for genes induced by ≥2-fold in SILP CD4^{+} T cells from *H. polygyrus*-rechallenged as compared to naïve *Bhlhe40*$^{+/+}$ mice. **(B)** Gene expression microarray data were analyzed for shared and unique Bhlhe40-dependent genes (≥2-fold differentially expressed) in SILP CD4^{+} T cells from naïve or *H. polygyrus*-rechallenged *Bhlhe40*$^{+/+}$ and *Bhlhe40*$^{-/-}$ mice, depicted as a Venn diagram. **(C)** Gene expression microarray data were analyzed for genes differentially expressed by ≥2-fold in SILP CD4^{+} T cells from naïve *Bhlhe40*$^{+/+}$ and *Bhlhe40*$^{-/-}$ mice. Microarray data are from a single experiment.

Figure S3. Bhlhe40 is required in T cells for normal cytokine production during *H. polygyrus* rechallenge. Related to Figure 4. (A and B) Naïve and *H. polygyrus*-rechallenged *Cd4-Cre*$^{-}$ *Bhlhe40*$^{fl/fl}$ and *Cd4-Cre*$^{+}$ *Bhlhe40*$^{fl/fl}$ mice were analyzed by flow cytometry for quantitation of the frequency of IL-4^{+}, IL-5^{+}, IL-13^{+}, and GM-CSF^{+} CD4^{+} T cells from the **(A)** peritoneal cavity and **(B)** mesenteric lymph nodes after *in vitro* PMA/ionomycin stimulation. Data are pooled from 2 independent experiments. Data are mean ± s.e.m. Significance calculated with an unpaired Student's *t*-test.

Figure S4. Further analysis of cytokine regulation during *H. polygyrus* rechallenge. Related to Figure 4. (A) Naïve and *H. polygyrus*-rechallenged *Cd4-Cre*$^{-}$ *Bhlhe40*$^{fl/fl}$ and *Cd4-Cre*$^{+}$ *Bhlhe40*$^{fl/fl}$ mice were analyzed by flow cytometry for quantitation of the frequency of IL-10^{+} CD4^{+} T cells after *in vitro* PMA/ionomycin stimulation of SILP cells. **(B)** *H. polygyrus*-rechallenged *Bhlhe40*$^{+/+}$, *Bhlhe40*$^{-/-}$, and *Bhlhe40*$^{-/-}$ *Il10*$^{-/-}$ mice were analyzed for quantitation of *H. polygyrus* eggs/gram feces over time. **(C)** Naïve and *H. polygyrus*-rechallenged *Bhlhe40*$^{+/+}$, *Bhlhe40*$^{-/-}$, and *Bhlhe40*$^{-/-}$ *Il10*$^{-/-}$ mice were analyzed for quantitation of intestinal granulomas. **(D)** *H. polygyrus*-rechallenged *Csf2*$^{+/+}$ and *Csf2*$^{-/-}$ mice were analyzed for quantitation of *H. polygyrus* eggs/gram feces over time. **(E)** Naïve and *H. polygyrus*-rechallenged *Csf2*$^{+/+}$ and *Csf2*$^{-/-}$ mice were analyzed for quantitation of intestinal granulomas. **(F)** Naïve and *H. polygyrus*-rechallenged *Csf2*$^{+/+}$ and *Csf2*$^{-/-}$ mice were analyzed by flow cytometry for quantitation of SILP myeloid cells. **(G-I)** Naïve and *H. polygyrus*-rechallenged *Csf2*$^{+/+}$ and *Csf2*$^{-/-}$ mice were analyzed by flow cytometry for quantitation of **(G)** peritoneal eosinophils, **(H)** LPMs, and **(I)** the frequency of RELMα^{+} LPMs. **(J)** Wild type mice were rechallenged with *H. polygyrus* concurrent with control rat polyclonal IgG or αGM-CSF antibody treatment and were analyzed for quantitation of *H. polygyrus* eggs/gram feces over time. **(K)** Naïve (hollow circles) and *H. polygyrus*-rechallenged mice (filled triangles) treated as in **(J)** were analyzed

for quantitation of intestinal granulomas. **(L)** Naïve (hollow circles) and *H. polygyrus*-rechallenged mice (filled triangles) treated as in **(J)** were analyzed by flow cytometry for quantitation of SILP myeloid cells. **(M-O)** Naïve and *H. polygyrus*-rechallenged *Csf2rb*$^{+/+}$ and *Csf2rb*$^{-/-}$ mice were analyzed by flow cytometry for quantitation of **(M)** peritoneal eosinophils, **(N)** LPMs, and **(O)** the frequency of RELMα^{+} LPMs. Data are pooled from 2 independent experiments **(A-C, M-O)** or are from single experiments **(D-L)**. Data are mean ± s.e.m. Significance calculated with an unpaired Student's *t*-test.

Methods

KEY RESOURCES TABLE

REAGENT or RESOURCE	SOURCE	IDENTIFIER
Antibodies		
α-smooth muscle actin (1A4) Cy3	Sigma	Cat# C6198; RRID:AB_476856
CD3ε (17A2) APC/Cy7	BioLegend	Cat# 100222
CD4 (RM4-5) PE/Cy7	BioLegend	Cat# 100528
CD4 (RM4-5) BV510	BioLegend	Cat# 100559
CD8a (53-6.7) PerCP/Cy5.5	Tonbo	Cat# 65-0081
CD8a (53-6.7) APC/Cy7	Tonbo	Cat# 25-0081
CD11b (M1/70) PE/Cy7	BioLegend, Tonbo	Cat# 101216, 60-0112
CD11b (M1/70) APC/Cy7	BioLegend, Tonbo	Cat# 101226, 25-0112
CD16/32 (2.4G2)	BioXCell	Cat# BE0008
CD19 (1D3) PerCP/Cy5.5	Tonbo	Cat# 65-0193
CD45 (30-F11) BV510	BD	Cat# 563891
CD45 (30-F11) RF710	Tonbo	Cat# 80-0451
CD45.2 (104) FITC	BioLegend	Cat# 109806
CD64 (X54-5/7.1) APC	BioLegend	Cat# 139306
CD102 (3C4) FITC	BioLegend	Cat# 105606
CD102 (3C4) AF647	BioLegend	Cat# 105612
CD115 (AFS98) PE	Tonbo	Cat# 50-1152
CD115 (AFS98) BV421	BioLegend	Cat# 135513
F4/80 (BM8) AF647	BioLegend	Cat# 123121
F4/80 (BM8.1) PerCP/Cy5.5	Tonbo	Cat# 65-4801
GM-CSF (MP1-22E9)	Leinco	Cat# G670; RRID:AB_2737496
GM-CSF (MP1-22E9) BV421	BD	Cat# 564747
Goat α-Rabbit AF647	Life Technologies	Cat# A21245
I-A/I-E (M5/114.15.2) BV510	BioLegend	Cat# 107635
I-A/I-E (M5/114.15.2) PB	BioLegend	Cat# 107620

I-A/I-E (M5/114.15.2) RF710	Tonbo	Cat# 80-5321
IL-4 (11B11) APC	BioLegend	Cat# 504105
IL-5 (11B11) BV421	BioLegend	Cat# 504311
IL-10 (JES5-16E3) APC	BioLegend	Cat# 505010
IL-13 (eBio 13A) PE/Cy7	eBioscience	Cat# 25-7133
Ly6C (HK1.4) APC/Cy7	BioLegend	Cat# 128026
Ly6C (HK1.4) BV510	BioLegend	Cat# 128033
Polyclonal rat IgG	Sigma	Cat# I4131
RELMα	Peprotech	Cat# 500-P214
Siglec-F (E50-2440) PE	BD	Cat# 552126
TCRβ (H57-597) PE	BioLegend	Cat# 109208
Bacterial and Virus Strains		
Heligmosomoides polygyrus bakeri	Joseph F. Urban, Jr., USDA Agricultural Research Service	Camberis et al. Curr Protoc Immunol, 2003.
Biological Samples		
Characterized Fetal Bovine Serum	HyClone and GE Healthcare	Cat# SH30396
Chemicals, Peptides, and Recombinant Proteins		
Fluoroshield mounting medium with DAPI	Abcam	Cat# ab104139
Pyrantel pamoate	Columbia Laboratories	NDC# 62337-415-16
Tissue Plus O.C.T. Compound	Fisher Healthcare	Cat# 4585
Phorbol 12-myristate 13-acetate (PMA)	Enzo Life Sciences	Cat# BML-PE160
Ionomycin calcium salt	Enzo Life Sciences	Cat# ALX-450-007
Brefeldin A	Enzo Life Sciences	Cat# BML-G405
Paraformaldehyde	Electron Microscopy Sciences	Cat# 15714
Bovine Serum Albumin	Fisher Bioreagents	Cat# BP1600-100
TMB Substrate Reagent Set	BD OptEIA	Cat# 555214
CAS-Block	Invitrogen	Cat # 008120
Collagenase from Clostridium histolyticum	Sigma	Cat# C5138
Critical Commercial Assays		
True-Nuclear Transcription Factor Buffer Set	BioLegend	Cat# 424401
Cytofix/Cytoperm	BD	Cat# 554714
E.Z.N.A. MicroElute Total RNA kit	Omega Bio-Tek	Cat# R6831
C57BL/6 Mouse Immunoglobulin Panel	SouthernBiotech	Cat# 5300-01B RRID:AB_2796077
Deposited Data		
Raw and analyzed data	Gene Expression Omnibus	Will be deposited after traditional publication
Experimental Models: Cell Lines		
NA		
Experimental Models: Organisms/Strains		
C57BL/6N	Taconic, bred in house	Cat# B6
C57BL/6J	Jackson	Cat# 000664
Il10-/- (B6.129P2-Il10tm1Cgn/J)	Jackson, crossed to Bhlhe40-/- in house	Cat# 002251

Csf2-/- (B6.129S-Csf2tm1Mlg/J)	Jackson	Cat# 026812
Csf2rb-/- (B6.129S1-Csf2rbtm1Cgb/J, Jackson)	Jackson, bred in house	Cat# 005940
Cd4-Cre (B6.Cg-Tg(Cd4-cre)1Cwi/BfluJ, Jackson)	Jackson, crossed to Bhlhe40fl/fl in house	Cat# 022071
LysM-Cre (B6N.129P2(B6)-Lyz2tm1(cre)Ifo/J)	Jackson, crossed to Bhlhe40fl/fl in house	Cat# 018956
Bhlhe40-/-	Backcrossed to B6 in house	Sun et al. Nat Immunol, 2001. Lin et al. Nat Comm, 2014.
Bhlhe40GFP+	GENSAT, Backcrossed to B6 in house	Lin et al. J Exp Med, 2016.
Bhlhe40fl/fl	KOMP, purchased from Jackson as Tm1a (no longer available). Bhlhe40fl/fl generated in ref.	Huynh et al. J Exp Med, 2018.
Oligonucleotides		
NA		
Recombinant DNA		
NA		
Software and Algorithms		
Arraystar	DNASTAR	Arraystar.com
Morpheus	Broad Institute	Software.broadinstitute.org/morpheme
Venn Diagram Plotter tool	Pacific Northwest National Laboratories	Omics.pnl.gov
GSEA	Broad Institute	Subramanian et al. Proc Natl Acad Sci U S A, 2005.
Prism 7 and 8	Graphpad	Graphpad.com
Illustrator CC	Adobe	Adobe.com
Photoshop CS6	Adobe	Adobe.com
Excel 2014	Microsoft	Microsoft.com
FACSDiva	BD	Bdbiosciences.com
FlowJo 7	Treestar	Flowjo.com
QCapture	QImaging	Qimaging.com
Other		
Two chamber McMaster counting slide	Chalex LLC	Vetslides.com

EXPERIMENTAL MODEL AND SUBJECT DETAILS

Mice

C57BL/6 (Taconic and Jackson), *Il10*$^{-/-}$ (B6.129P2-Il10tm1Cgn/J, Jackson), *Csf2*$^{-/-}$ (B6.129S-*Csf2*^{tm1Mlg}/J, Jackson), *Csf2rb*$^{-/-}$ (B6.129S1-*Csf2rb*^{tm1Cgb}/J, Jackson), *Cd4-Cre* (B6.Cg-Tg(Cd4-cre)1Cwi/BfluJ, Jackson) and *LysM-Cre* (B6N.129P2(B6)-*Lyz2*$^{tm1(cre)Ifo}$/J, Jackson) mice were

obtained from the vendors listed. *Bhlhe40*$^{-/-}$ (10 generations backcrossed to the C57BL/6 background) (Lin et al., 2014; Sun et al., 2001), *Bhlhe40*$^{GFP+}$ (10 generations backcrossed to the C57BL/6 background) (Lin et al., 2016), and *Bhlhe40*$^{fl/fl}$ (Huynh et al., 2018) mice have been previously reported. All mice were maintained in our specific pathogen free animal facility. Sex-matched littermates were used for experiments whenever possible. Experiments with *Csf2*$^{-/-}$ and *Csf2rb*$^{-/-}$ mice used cohoused, age-matched, sex-matched C57BL/6 controls bred in our animal facility or purchased from Jackson. All animal experiments were approved by the Animal Studies Committee of Washington University in St. Louis.

METHOD DETAILS

Heligmosomoides polygyrus bakeri infections

Infective *Heligmosomoides polygyrus bakeri* third-stage larvae (L3) were prepared as described (Camberis et al., 2003). For both primary and secondary infection, mice were orally gavaged with 200 L3 with a 20-gauge ball-tipped gavage needle. Female mice were used for experiments whenever possible. Fecal samples were collected at 8, 11, 14, and 21 days after primary and secondary infection and weighed. Eggs were counted by dissolution of feces in 5 ml water, followed by a 1:1 dilution with a saturated sodium chloride solution before loading into a McMaster counting chamber (Chalex LLC). For rechallenge experiments, mice were cleared of infection by oral gavage with 2 mg of pyrantel pamoate (Columbia Laboratories) diluted in Dulbecco's PBS on days 14 and 15 after primary infection and were rested for 3-4 weeks before reinfection. Blood was collected at day 21 post-rechallenge and allowed to clot for >1 hour before serum collection by centrifugation at 1,500 g for 15 minutes. Mice were sacrificed on day 17 or 22 of secondary infection for assessment of cellular responses. Macroscopic granulomas present at day 22 of secondary infection that were visible to the naked eye were counted along the length of the intact intestines. Assessment of the intestinal worm burden was performed at day 17 or 22 of primary or secondary infection. Adult worms were collected by cutting the

intestine open and into ~4 in sections, placing the tissue and contents into a metal filter on top of a 50 ml tube of PBS, and setting the tube in a 37 ºC water bath. Worms then actively migrated through the filter over several hours and sedimented. Worms were counted visually in petri dishes.

In vivo antibody blockade

Mice were infected, cleared, and rested as above. Immediately before reinfection, mice were injected i.p. with 300 µg of αGM-CSF (Leinco, G670, clone MP1-22E9) or control polyclonal rat IgG (Sigma Aldrich, I4131) and were given the same dose i.p. every other day until sacrifice (Codarri et al., 2011).

Enzyme-linked immunosorbent assay (ELISA)

Adult worms collected as above were washed repeatedly in PBS, and ground in a Dounce homogenizer in 1 mL of PBS. Debris was then pelleted by centrifugation at 16,000 g for 20 minutes at 4 ºC. The supernatant was passed through a 0.2 µm filter and stored at -80 ºC. Lysate was titrated for an ELISA with the serum of *H. polygyrus*-rechallenged mice, and the greatest dilution of lysate (1:1000) which yielded maximal signal was used. Nunc Maxisorp plates were coated with *H. polygyrus* lysate overnight. Wells were washed with PBS-Tween 20 (0.05%), and 1% BSA in PBS was added for one hour to block. After washing, serum was added for two hours. After washing, anti-IgG1 antibody conjugated to horseradish peroxidase (from the SouthernBiotech C57BL/6 Mouse Immunoglobulin Panel (5300-01B)) was added for one hour. After washing, a 1:1 mixture of room temperature TMB A and B solutions (BD OptEIA) was added for ~1-2 minutes. The reaction was stopped with 1 M H_3PO_4. Samples were analyzed on an iMark microplate reader (BioRad). Serum was diluted between 10^{-2} and 10^{-8} and the last well with an OD_{450} above 0.100 represented the titer.

Brightfield and epifluorescence microscopy

The proximal 6 cm of the small intestine were formed into a swiss roll (Bialkowska et al., 2016) and were frozen in OCT media. 10 μm cryosections were cut using a Leica CM1950 cryostat. For hematoxylin and eosin staining, sections were fixed in 4% PFA, washed, and stained. For immunofluorescent staining, sections were fixed in acetone, washed, and blocked with CAS-Block (Invitrogen). Staining was performed with Cy3-anti-α-smooth muscle actin (clone 1A4, Sigma) and AlexaFluor647-anti-F4/80 (clone BM8, BioLegend) diluted in CAS block, followed by washing. Sections were mounted with Abcam Fluoroshield Mounting Medium with DAPI. All images were captured with a Nikon Eclipse E800 microscope equipped with a MicroPublisher 5.0 RTV camera (QImaging) for brightfield microscopy and an EXi Blue camera (QImaging) for fluorescence microscopy using QCapture software (QImaging). Fluorescence images were merged and levelled in Adobe Photoshop.

Leukocyte collection from tissues

Peritoneal cells were collected from body cavities by lavage. Mesenteric lymph nodes were harvested into IMDM (with added FBS, L-glutamine, sodium pyruvate, non-essential amino acids, penicillin/streptomycin, and β-mercaptoethanol), homogenized through a 70 μm filter, and washed. Isolation of small intestine lamina propria cells was performed as described (Bando et al., 2018). In brief, 4 cm of the proximal small intestine were excised, cleaned of fecal contents, and cut into 2-3 pieces. The tissue was shaken twice in 1x HBSS (with added HEPES, FBS, EDTA, and DTT) for 20 minutes to remove the epithelial layer. The tissue was then shaken at 220 rpm at 37 ºC for 1 hour in an Innova 4330 shaker (New Brunswick Scientific) with Collagenase IV (Sigma, C5138) in RPMI 1640 (with added L-glutamine, penicillin/streptomycin, 2-mercaptoethanol, and FBS). Cells were then pelleted by centrifugation and washed.

All cells were passed through a 70 μm cell strainer before analysis. If necessary, tissues were treated with ACK lysis buffer to lyse red blood cells. Cells were counted with a

hemocytometer using trypan blue.

Flow cytometry

Cell surface staining was conducted in PBS with 0.5% BSA and 2 mM EDTA (hereafter FACS buffer) with or without 0.02% sodium azide. In brief, cells were washed in FACS buffer, blocked with α-CD16/32 (clone 2.4G2, BioXCell) for 5-10 minutes at 4 ºC, stained for 20 minutes at 4 ºC, and washed with FACS buffer before flow cytometry. Flow cytometry was performed on LSRFortessa X20, FACSCanto II, and LSR II instruments (all BD). Analysis was performed with FlowJo software (Treestar). Antibodies and fluorescent dyes used in this study are listed under Key Resources.

Gating of cell populations was as follows (all analysis pre-gated on FSC/SSC followed by a FSC-W/FSC-A singlet gate). SILP macrophages were gated as $CD45^+F4/80^+CD64^+MHC\text{-}II^+Ly6C^-$, while GMMs were gated as $CD45^+F4/80^+CD64^+MHC\text{-}II^{lo}Ly6C^{lo}$. SILP eosinophils were gated as $CD45^+F4/80^+CD64^-CD11b^+SSC\text{-}A^{hi}$, and this approach was validated in some experiments with Siglec-F staining. SILP $CD3^+$ T cells were gated as $CD45^+F4/80^-CD64^-CD19^-CD3^+$. SILP $CD4^+$ T cells were gated as $CD19^-F4/80^-TCR\beta^+CD4^+CD8^-$. LPMs were gated as $CD115^+CD11b^+ICAM2^+MHC\text{-}II^{lo}$. Peritoneal eosinophils were gated as $Siglec\text{-}F^+ICAM2^-$. Peritoneal $CD4^+$ T cells were gated as $ICAM2^-TCR\beta^+CD4^+CD8^-$. Mesenteric lymph node $CD4^+$ T cells were gated as $CD19^-TCR\beta^+CD4^+CD8^-$.

Intracellular staining for flow cytometry

For intracellular cytokine staining of T cells, total SILP, peritoneal, and mesenteric lymph node cells were cultured at 0.5-1 million cells/well in a 96 well V-bottom non-tissue culture-treated plate for 3-4 hours at 37 °C with 8% CO_2 in the presence of PMA (50 ng/ml), ionomycin (1 μM), and brefeldin A (1 μg/ml) in IMDM (with added FBS, L-glutamine, sodium pyruvate, non-essential amino acids, penicillin/streptomycin, and β-mercaptoethanol). Cells were then surface

stained and fixed with 4% paraformaldehyde (PFA). Cells were then washed with FACS buffer and stored overnight. To permeabilize the cells, samples were washed with 1x Perm/Wash buffer (BD, 554714) and stained for 20 minutes at 4 ºC, followed by washing in 1x Perm/Wash buffer and FACS buffer before flow cytometry.

For RELMα staining, the BioLegend True-Nuclear Transcription Factor Buffer set (424401) was used. After surface staining, cells were fixed with 1x Fix Concentrate buffer in Fix Diluent for 30 minutes at 4 ºC. Cells were then washed with FACS buffer and stored overnight. Samples were washed with 1x Perm buffer diluted in water for permeabilization. After blocking with 2% rat serum, samples were stained for 1 hour at RT with anti-RELMα antibody followed by washing in 1x Perm buffer, staining with secondary antibody for 20 min at 4 ºC, washing in 1x Perm buffer, and washing in FACS buffer before flow cytometry.

Microarrays

Singlet F4/80$^-$ TCRβ$^+$ CD4$^+$ CD8$^-$ SILP cells were sorted from naïve and *H. polygyrus*-rechallenged mice using a FACSAria II (BD) into FBS, followed by lysis and RNA purification using the E.Z.N.A. MicroElute Total RNA kit (Omega Bio-Tek). RNA was submitted to the Genome Technology Access core at Washington University for cDNA synthesis (NuGen Pico SL) followed by analysis on the Affymetrix Mouse Gene 1.0 ST microarray platform. Data were analyzed with the DNASTAR ArrayStar program. All CEL files were normalized together. Genes with an expression value of >5 (in log 2 scale) in at least one replicate were considered expressed. For generation of lists of differentially expressed genes at a ≥2-fold differential expression cutoff between groups, p-value significance of ≤0.01 by the moderated *t*-test was also required. Morpheus was used to generate heatmaps (software.broadinstitute.org/morpheus/). The Venn Diagram Plotter tool (Pacific Northwest National Laboratories, omics.pnl.gov) was used to generate Venn diagrams. Multiple differentially expressed probe sets representing a single gene were presented in heat maps, but

only unique genes were counted in Venn diagrams. To assess gene set enrichment, the GSEA software from the Broad Institute was used to analyze all expressed genes for enrichment of C5 database gene sets (Subramanian et al., 2005).

QUANTIFICATION AND STATISTICAL ANALYSIS

All data are from at least two independent experiments, unless otherwise indicated. Data were analyzed by unpaired two-tailed Student's *t*-tests (Prism 7; GraphPad Software, Inc.) with $p \leq 0.05$ considered significant. For relevant comparisons where no p-value is shown, the p-value was > 0.05. The NES score calculated by the GSEA software was used to account for set size effects when determining enrichment of gene sets. The GSEA-calculated FWER p value was used as a conservative measure of significance. Horizontal bars represent the mean and error bars represent the standard error of the mean (s.e.m.).

References

1. Allen, J.E., and Sutherland, T.E. (2014). Host protective roles of type 2 immunity: parasite killing and tissue repair, flip sides of the same coin. Semin. Immunol. *26*, 329-340.
2. Anthony, R.M., Urban, J.F., Alem, F., Hamed, H.A., Rozo, C.T., Boucher, J.L., Van Rooijen, N., and Gause, W.C. (2006). Memory T(H)2 cells induce alternatively activated macrophages to mediate protection against nematode parasites. Nat. Med. *12*, 955-960.
3. Bagnasco, D., Ferrando, M., Varricchi, G., Puggioni, F., Passalacqua, G., and Canonica, G.W. (2017). Anti-Interleukin 5 (IL-5) and IL-5Ra Biological Drugs: Efficacy, Safety, and Future Perspectives in Severe Eosinophilic Asthma. Front. Med. (Lausanne) *4*, 135.
4. Bain, C.C., Bravo-Blas, A., Scott, C.L., Perdiguero, E.G., Geissmann, F., Henri, S., Malissen, B., Osborne, L.C., Artis, D., and Mowat, A.M. (2014). Constant replenishment

from circulating monocytes maintains the macrophage pool in the intestine of adult mice. Nat. Immunol. *15*, 929-937.

5. Bando, J.K., Gilfillan, S., Song, C., McDonald, K.G., Huang, S.C., Newberry, R.D., Kobayashi, Y., Allan, D.S.J., Carlyle, J.R., Cella, M., and Colonna, M. (2018). The Tumor Necrosis Factor Superfamily Member RANKL Suppresses Effector Cytokine Production in Group 3 Innate Lymphoid Cells. Immunity *48*, 1208-1219.e1204.
6. Becher, B., Tugues, S., and Greter, M. (2016). GM-CSF: From Growth Factor to Central Mediator of Tissue Inflammation. Immunity *45*, 963-973.
7. Bialkowska, A.B., Ghaleb, A.M., Nandan, M.O., and Yang, V.W. (2016). Improved Swiss-rolling Technique for Intestinal Tissue Preparation for Immunohistochemical and Immunofluorescent Analyses. J. Vis. Exp. *113*, e54161.
8. Camberis, M., Le Gros, G., and Urban, J., Jr. (2003). Animal model of Nippostrongylus brasiliensis and Heligmosomoides polygyrus. Curr. Protoc. Immunol. *Chapter 19*, Unit 19.12.
9. Camponeschi, A., Todi, L., Cristofoletti, C., Lazzeri, C., Carbonari, M., Mitrevski, M., Marrapodi, R., Del Padre, M., Fiorilli, M., Casato, M., and Visentini, M. (2018). DEC1/STRA13 is a key negative regulator of activation-induced proliferation of human B cells highly expressed in anergic cells. Immunol. Lett. *198*, 7-11.
10. Cates, E.C., Fattouh, R., Wattie, J., Inman, M.D., Goncharova, S., Coyle, A.J., Gutierrez-Ramos, J.C., and Jordana, M. (2004). Intranasal exposure of mice to house dust mite elicits allergic airway inflammation via a GM-CSF-mediated mechanism. J. Immunol. *173*, 6384-6392.
11. Chen, T., Tibbitt, C.A., Feng, X., Stark, J.M., Rohrbeck, L., Rausch, L., Sedimbi, S.K., Karlsson, M.C.I., Lambrecht, B.N., Karlsson Hedestam, G.B., et al. (2017). PPAR-gamma promotes type 2 immune responses in allergy and nematode infection. Sci. Immunol. *2*, eaal5196.

12. Chenery, A.L., Alhallaf, R., Agha, Z., Ajendra, J., Parkinson, J., Cooper, M.M., Chan, B.H.K., Eichenberger, R.M., Dent, L.A., Robertson, A.A.B., et al. (2019). Inflammasome-independent role for NLRP3 in controlling innate anti-helminth immunity and tissue repair in the lung. BioRxiv, 10.1101/606392.
13. Codarri, L., Gyulveszi, G., Tosevski, V., Hesske, L., Fontana, A., Magnenat, L., Suter, T., and Becher, B. (2011). RORgammat drives production of the cytokine GM-CSF in helper T cells, which is essential for the effector phase of autoimmune neuroinflammation. Nat. Immunol. *12*, 560-567.
14. Croxford, A.L., Lanzinger, M., Hartmann, F.J., Schreiner, B., Mair, F., Pelczar, P., Clausen, B.E., Jung, S., Greter, M., and Becher, B. (2015). The Cytokine GM-CSF Drives the Inflammatory Signature of CCR2+ Monocytes and Licenses Autoimmunity. Immunity *43*, 502-514.
15. Deepe, G.S., Jr., Gibbons, R., and Woodward, E. (1999). Neutralization of endogenous granulocyte-macrophage colony-stimulating factor subverts the protective immune response to Histoplasma capsulatum. J. Immunol. *163*, 4985-4993.
16. Dougan, M., Dranoff, G., and Dougan, S.K. (2019). GM-CSF, IL-3, and IL-5 Family of Cytokines: Regulators of Inflammation. Immunity *50*, 796-811.
17. Esnault, S., and Kelly, E.A. (2016). Essential Mechanisms of Differential Activation of Eosinophils by IL-3 Compared to GM-CSF and IL-5. Crit. Rev. Immunol. *36*, 429-444.
18. Filbey, K.J., Grainger, J.R., Smith, K.A., Boon, L., van Rooijen, N., Harcus, Y., Jenkins, S., Hewitson, J.P., and Maizels, R.M. (2014). Innate and adaptive type 2 immune cell responses in genetically controlled resistance to intestinal helminth infection. Immunol. Cell Biol. *92*, 436-448.
19. Gabrysova, L., Alvarez-Martinez, M., Luisier, R., Cox, L.S., Sodenkamp, J., Hosking, C., Perez-Mazliah, D., Whicher, C., Kannan, Y., Potempa, K., et al. (2018). c-Maf controls

immune responses by regulating disease-specific gene networks and repressing IL-2 in CD4(+) T cells. Nat. Immunol. *19*, 497-507.

20. Gonzalez-Juarrero, M., Hattle, J.M., Izzo, A., Junqueira-Kipnis, A.P., Shim, T.S., Trapnell, B.C., Cooper, A.M., and Orme, I.M. (2005). Disruption of granulocyte macrophage-colony stimulating factor production in the lungs severely affects the ability of mice to control Mycobacterium tuberculosis infection. J. Leukoc. Biol. *77*, 914-922.
21. Henriksson, J., Chen, X., Gomes, T., Ullah, U., Meyer, K.B., Miragaia, R., Duddy, G., Pramanik, J., Yusa, K., Lahesmaa, R., and Teichmann, S.A. (2019). Genome-wide CRISPR Screens in T Helper Cells Reveal Pervasive Crosstalk between Activation and Differentiation. Cell *176*, 882-896.e18.
22. Herbst, T., Esser, J., Prati, M., Kulagin, M., Stettler, R., Zaiss, M.M., Hewitson, J.P., Merky, P., Verbeek, J.S., Bourquin, C., et al. (2012). Antibodies and IL-3 support helminth-induced basophil expansion. Proc. Natl. Acad. Sci. U. S. A. *109*, 14954-14959.
23. Hirata, Y., Egea, L., Dann, S.M., Eckmann, L., and Kagnoff, M.F. (2010). GM-CSF-facilitated dendritic cell recruitment and survival govern the intestinal mucosal response to a mouse enteric bacterial pathogen. Cell Host Microbe *7*, 151-163.
24. Huynh, J.P., Lin, C.C., Kimmey, J.M., Jarjour, N.N., Schwarzkopf, E.A., Bradstreet, T.R., Shchukina, I., Shpynov, O., Weaver, C.T., Taneja, R., et al. (2018). Bhlhe40 is an essential repressor of IL-10 during Mycobacterium tuberculosis infection. J. Exp. Med. *215*, 1823-1838.
25. Jarjour, N.N., Schwarzkopf, E.A., Bradstreet, T.R., Shchukina, I., Lin, C.C., Huang, S.C., Lai, C.W., Cook, M.E., Taneja, R., Stappenbeck, T.S., et al. (2019). Bhlhe40 mediates tissue-specific control of macrophage proliferation in homeostasis and type 2 immunity. Nat. Immunol. *20*, 687-700.
26. Kanda, M., Yamanaka, H., Kojo, S., Usui, Y., Honda, H., Sotomaru, Y., Harada, M., Taniguchi, M., Suzuki, N., Atsumi, T., et al. (2016). Transcriptional regulator Bhlhe40

works as a cofactor of T-bet in the regulation of IFN-γ production in iNKT cells. Proc. Natl. Acad. Sci. U. S. A. *113*, E3394-3402.

27. Kreslavsky, T., Vilagos, B., Tagoh, H., Poliakova, D.K., Schwickert, T.A., Wohner, M., Jaritz, M., Weiss, S., Taneja, R., Rossner, M.J., and Busslinger, M. (2017). Essential role for the transcription factor Bhlhe41 in regulating the development, self-renewal and BCR repertoire of B-1a cells. Nat. Immunol. *18*, 442-455.
28. LeVine, A.M., Reed, J.A., Kurak, K.E., Cianciolo, E., and Whitsett, J.A. (1999). GM-CSF–deficient mice are susceptible to pulmonary group B streptococcal infection. J. Clin. Invest. *103*, 563-569.
29. Lin, C.C., Bradstreet, T.R., Schwarzkopf, E.A., Jarjour, N.N., Chou, C., Archambault, A.S., Sim, J., Zinselmeyer, B.H., Carrero, J.A., Wu, G.F., et al. (2016). IL-1-induced Bhlhe40 identifies pathogenic T helper cells in a model of autoimmune neuroinflammation. J. Exp. Med. *213*, 251-271.
30. Lin, C.C., Bradstreet, T.R., Schwarzkopf, E.A., Sim, J., Carrero, J.A., Chou, C., Cook, L.E., Egawa, T., Taneja, R., Murphy, T.L., et al. (2014). Bhlhe40 controls cytokine production by T cells and is essential for pathogenicity in autoimmune neuroinflammation. Nat. Commun. *5*, 3551.
31. Maizels, R.M., and Balic, A. (2004). Resistance to Helminth Infection: The Case for Interleukin-5-Dependent Mechanisms. J. Infect. Dis. *190*, 427-429.
32. Maizels, R.M., Smits, H.H., and McSorley, H.J. (2018). Modulation of Host Immunity by Helminths: The Expanding Repertoire of Parasite Effector Molecules. Immunity *49*, 801-818.
33. Mandujano, J.F., D'Souza, N.B., Nelson, S., Summer, W.R., Beckerman, R.C., and Shellito, J.E. (1995). Granulocyte-macrophage colony stimulating factor and Pneumocystis carinii pneumonia in mice. Am. J. Respir. Crit. Care Med. *151*, 1233-1238.

34. Martínez-Llordella, M., Esensten, J.H., Bailey-Bucktrout, S.L., Lipsky, R.H., Marini, A., Chen, J., Mughal, M., Mattson, M.P., Taub, D.D., and Bluestone, J.A. (2013). CD28-inducible transcription factor DEC1 is required for efficient autoreactive CD4+ T cell response. J. Exp. Med. *210*, 1603-1619.
35. Massacand, J.C., Stettler, R.C., Meier, R., Humphreys, N.E., Grencis, R.K., Marsland, B.J., and Harris, N.L. (2009). Helminth products bypass the need for TSLP in Th2 immune responses by directly modulating dendritic cell function. Proc. Natl. Acad. Sci. U. S. A. *106*, 13968-13973.
36. Mohrs, K., Harris, D.P., Lund, F.E., and Mohrs, M. (2005). Systemic dissemination and persistence of Th2 and type 2 cells in response to infection with a strictly enteric nematode parasite. J. Immunol. *175*, 5306-5313.
37. Nobs, S.P., Natali, S., Pohlmeier, L., Okreglicka, K., Schneider, C., Kurrer, M., Sallusto, F., and Kopf, M. (2017). PPARgamma in dendritic cells and T cells drives pathogenic type-2 effector responses in lung inflammation. J. Exp. Med. *214*, 3015-3035.
38. Paine, R., 3rd, Preston, A.M., Wilcoxen, S., Jin, H., Siu, B.B., Morris, S.B., Reed, J.A., Ross, G., Whitsett, J.A., and Beck, J.M. (2000). Granulocyte-macrophage colony-stimulating factor in the innate immune response to Pneumocystis carinii pneumonia in mice. J. Immunol. *164*, 2602-2609.
39. Patel, N., Kreider, T., Urban, J.F., Jr., and Gause, W.C. (2009). Characterisation of effector mechanisms at the host:parasite interface during the immune response to tissue-dwelling intestinal nematode parasites. Int. J. Parasitol. *39*, 13-21.
40. Pei, C., Zhao, C., Wang, A.J., Fan, A.X., Grinchuk, V., Smith, A., Sun, R., Xie, Y., Lu, N., Urban, J.F., Jr., et al. (2016). Critical Role for Interleukin-25 in Host Protective Th2 Memory Response against Heligmosomoides polygyrus bakeri. Infect. Immun. *84*, 3328-3337.

41. Robb, L., Drinkwater, C.C., Metcalf, D., Li, R., Kontgen, F., Nicola, N.A., and Begley, C.G. (1995). Hematopoietic and lung abnormalities in mice with a null mutation of the common beta subunit of the receptors for granulocyte-macrophage colony-stimulating factor and interleukins 3 and 5. Proc. Natl. Acad. Sci. U. S. A. *92*, 9565-9569.
42. Roufosse, F. (2018). Targeting the Interleukin-5 Pathway for Treatment of Eosinophilic Conditions Other than Asthma. Front. Med. (Lausanne) *5*, 49.
43. Schwartz, C., Turqueti-Neves, A., Hartmann, S., Yu, P., Nimmerjahn, F., and Voehringer, D. (2014). Basophil-mediated protection against gastrointestinal helminths requires IgE-induced cytokine secretion. Proc. Natl. Acad. Sci. U. S. A. *111*, E5169-5177.
44. Scott, C.L., Bain, C.C., and Mowat, A.M. (2017). Isolation and Identification of Intestinal Myeloid Cells. Methods Mol. Biol. *1559*, 223-239.
45. Seimiya, M., Wada, A., Kawamura, K., Sakamoto, A., Ohkubo, Y., Okada, S., Hatano, M., Tokuhisa, T., Watanabe, T., Saisho, H., et al. (2004). Impaired lymphocyte development and function in Clast5/Stra13/DEC1-transgenic mice. Eur. J. Immunol. *34*, 1322-1332.
46. Sheih, A., Parks, W.C., and Ziegler, S.F. (2017). GM-CSF produced by the airway epithelium is required for sensitization to cockroach allergen. Mucosal Immunol. *10*, 705-715.
47. Shim, D.S., Schilter, H.C., Knott, M.L., Almeida, R.A., Short, R.P., Mackay, C.R., Dent, L.A., and Sewell, W.A. (2012). Protection against Nippostrongylus brasiliensis infection in mice is independent of GM-CSF. Immunol. Cell Biol. *90*, 553-558.
48. Sorobetea, D., Svensson-Frej, M., and Grencis, R. (2018). Immunity to gastrointestinal nematode infections. Mucosal Immunol. *11*, 304-315.

49. Steinfelder, S., Rausch, S., Michael, D., Kuhl, A.A., and Hartmann, S. (2017). Intestinal helminth infection induces highly functional resident memory CD4(+) T cells in mice. Eur. J. Immunol. *47*, 353-363.

50. Subramanian, A., Tamayo, P., Mootha, V.K., Mukherjee, S., Ebert, B.L., Gillette, M.A., Paulovich, A., Pomeroy, S.L., Golub, T.R., Lander, E.S., and Mesirov, J.P. (2005). Gene set enrichment analysis: a knowledge-based approach for interpreting genome-wide expression profiles. Proc. Natl. Acad. Sci. U. S. A. *102*, 15545-15550.

51. Sun, H., Lu, B., Li, R.Q., Flavell, R.A., and Taneja, R. (2001). Defective T cell activation and autoimmune disorder in Stra13-deficient mice. Nat. Immunol. *2*, 1040-1047.

52. Tibbit, C.A., Stark, J.M., Martens, L., Ma, J., Mold, J.E., Deswarte, K., Oliynyk, G., Feng, X., Lambrecht, B.N., De Bleser, P., et al. (2019). Single-Cell RNA Sequencing of the T Helper Cell Response to House Dust Mites Defines a Distinct Gene Expression Signature in Airway Th2 Cells. Immunity *51*, 1-16.

53. Urban, J.F., Jr., Katona, I.M., Paul, W.E., and Finkelman, F.D. (1991). Interleukin 4 is important in protective immunity to a gastrointestinal nematode infection in mice. Proc. Natl. Acad. Sci. U. S. A. *88*, 5513-5517.

54. Yamashita, N., Tashimo, H., Ishida, H., Kaneko, F., Nakano, J., Kato, H., Hirai, K., Horiuchi, T., and Ohta, K. (2002). Attenuation of airway hyperresponsiveness in a murine asthma model by neutralization of granulocyte-macrophage colony-stimulating factor (GM-CSF). Cell. Immunol. *219*, 92-97.

55. Yasuda, K., Kitagawa, Y., Kawakami, R., Isaka, Y., Watanabe, H., Kondoh, G., Kohwi-Shigematsu, T., Sakaguchi, S., and Hirota, K. (2019). Satb1 regulates the effector program of encephalitogenic tissue Th17 cells in chronic inflammation. Nat. Commun. *10*, 549.

56. Yu, F., Sharma, S., Jankovic, D., Gurram, R.K., Su, P., Hu, G., Li, R., Rieder, S., Zhao, K., Sun, B., and Zhu, J. (2018). The transcription factor Bhlhe40 is a switch of

inflammatory versus antiinflammatory Th1 cell fate determination. J. Exp. Med. *215*, 1813-1821.

57. Zaiss, D.M., Yang, L., Shah, P.R., Kobie, J.J., Urban, J.F., and Mosmann, T.R. (2006). Amphiregulin, a TH2 cytokine enhancing resistance to nematodes. Science *314*, 1746.
58. Zaiss, M.M., Maslowski, K.M., Mosconi, I., Guenat, N., Marsland, B.J., and Harris, N.L. (2013). IL-1beta suppresses innate IL-25 and IL-33 production and maintains helminth chronicity. PLoS Pathog. *9*, e1003531.
59. Zhan, Y., Lieschke, G.J., Grail, D., Dunn, A.R., and Cheers, C. (1998). Essential roles for granulocyte-macrophage colony-stimulating factor (GM-CSF) and G-CSF in the sustained hematopoietic response of Listeria monocytogenes-infected mice. Blood *91*, 863-869.

Figure 1: Bhlhe40 is required for a protective recall response to *H. polygyrus*

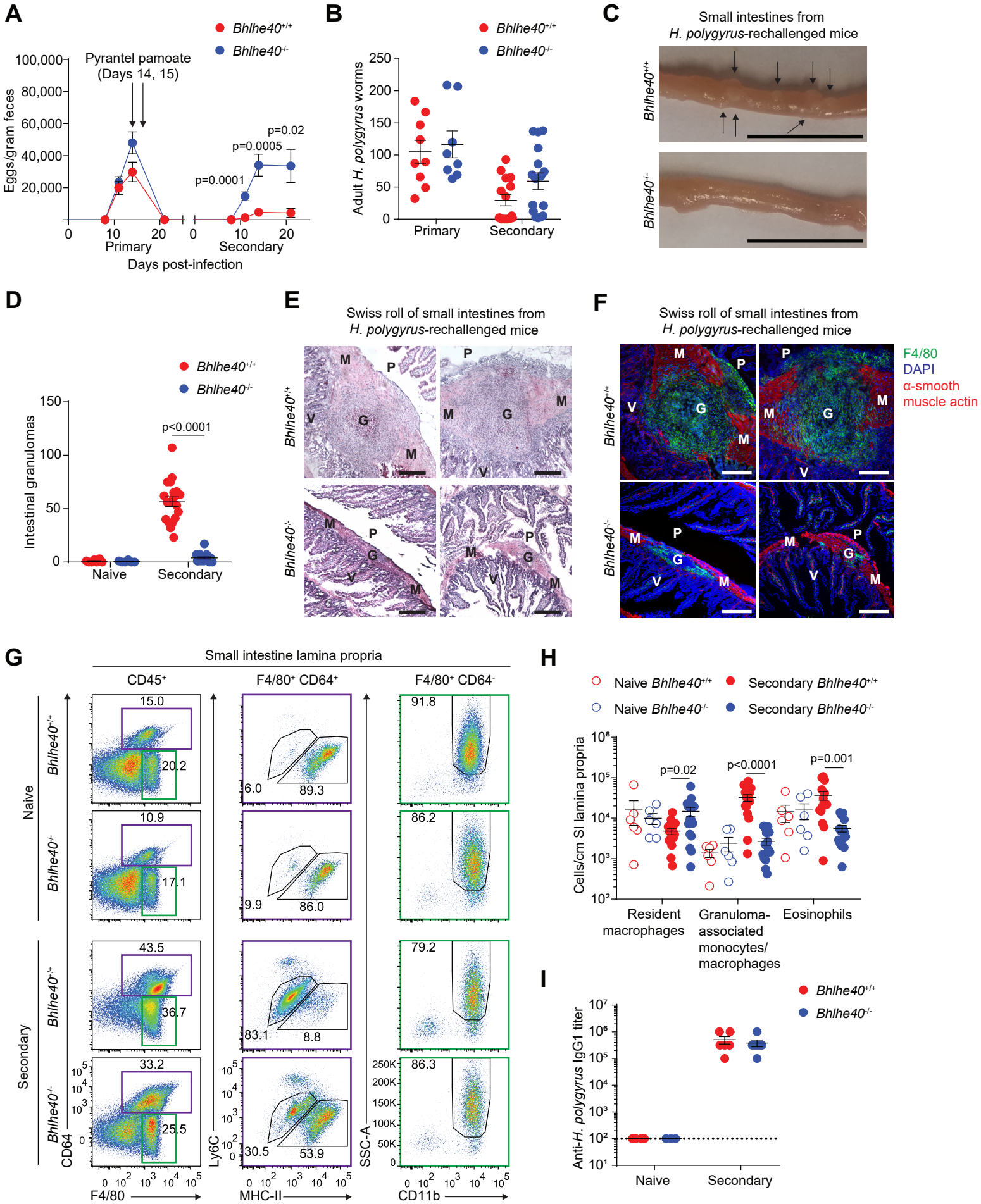

Figure 2: Bhlhe40 is required in T cells for a normal memory response to *H. polygyrus*

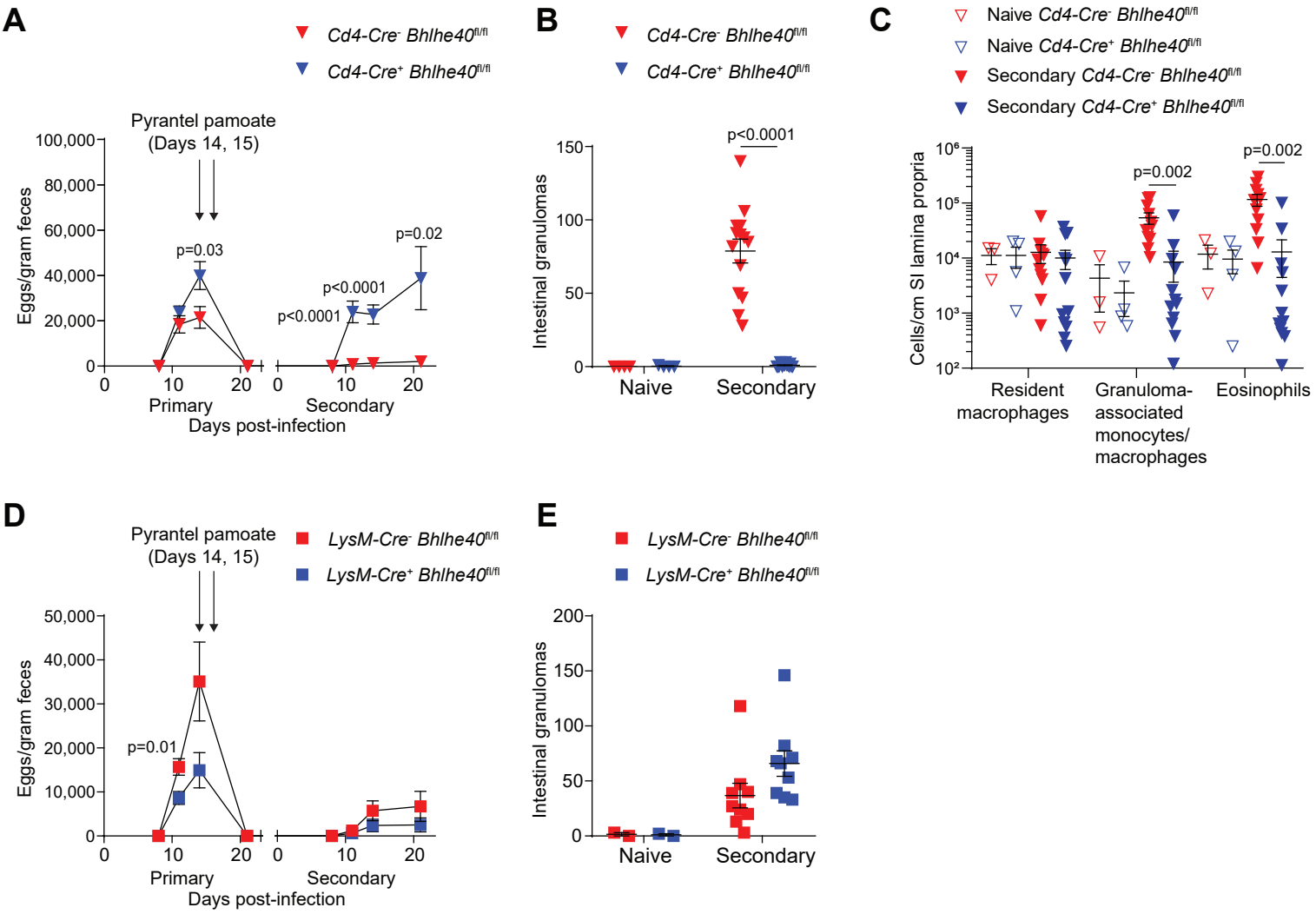

Figure 3: Loss of Bhlhe40 dysregulates the CD4⁺ T cell transcriptional response to *H. polygyrus* rechallenge

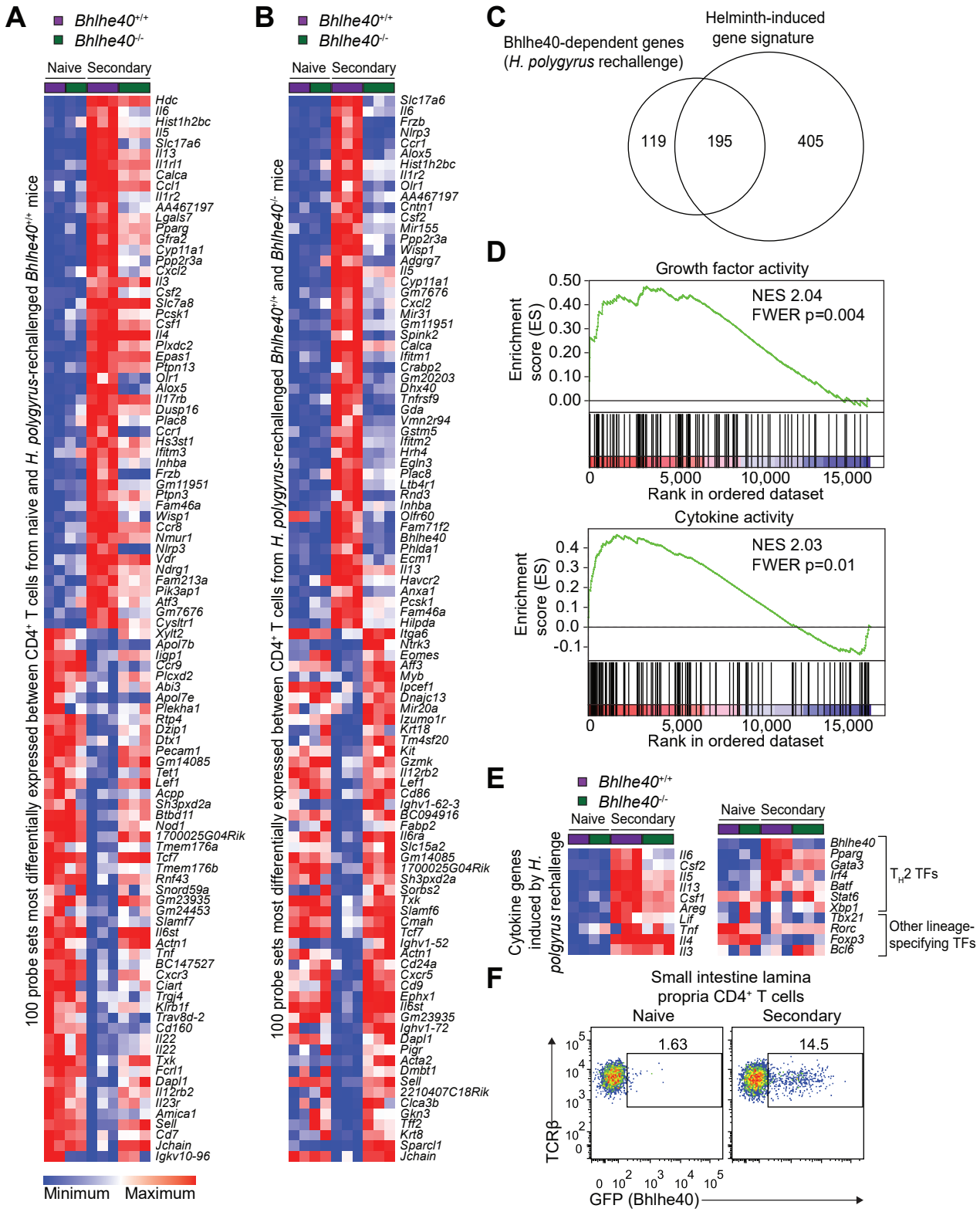

Figure 4: Bhlhe40 is required for normal CD4⁺ T cell production of β_c chain-dependent cytokines necessary for control of *H. polygyrus* rechallenge

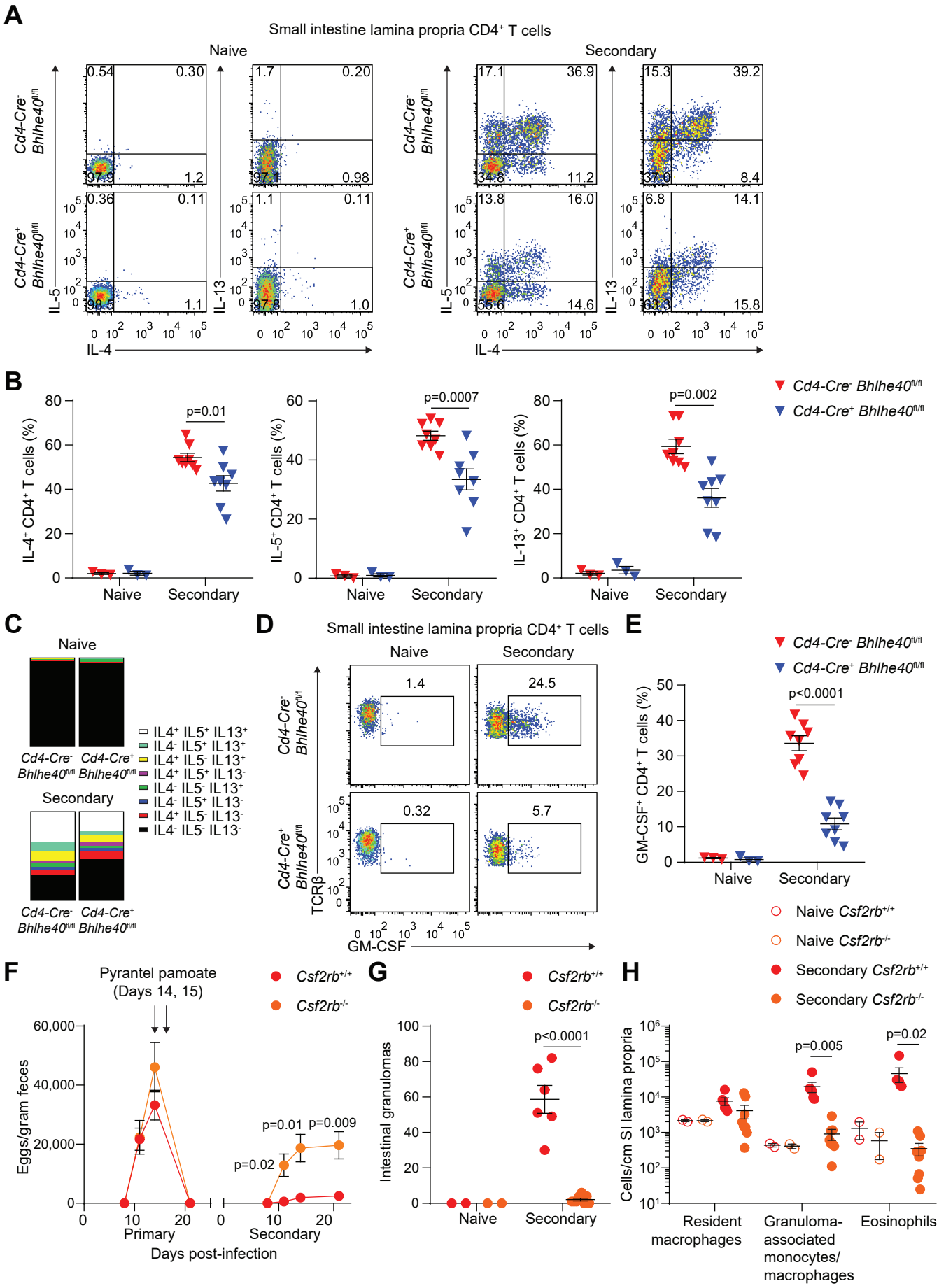

Figure S1: Loss of Bhlhe40 dysregulates myeloid cell responses to *H. polygyrus* rechallenge

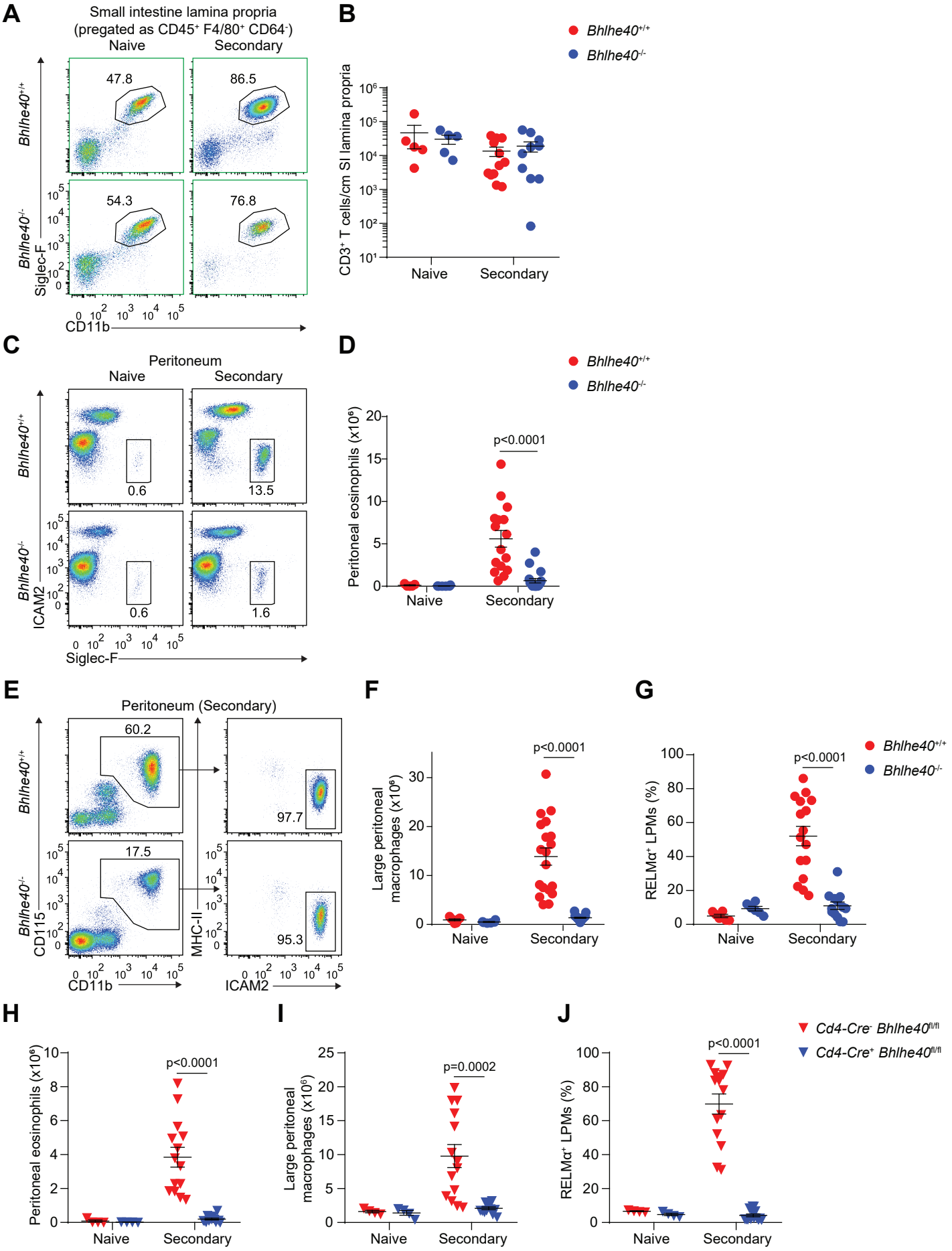

Figure S2: Bhlhe40 regulates distinct gene sets in CD4⁺ T cells from naive and *H. polygyrus*-rechallenged mice

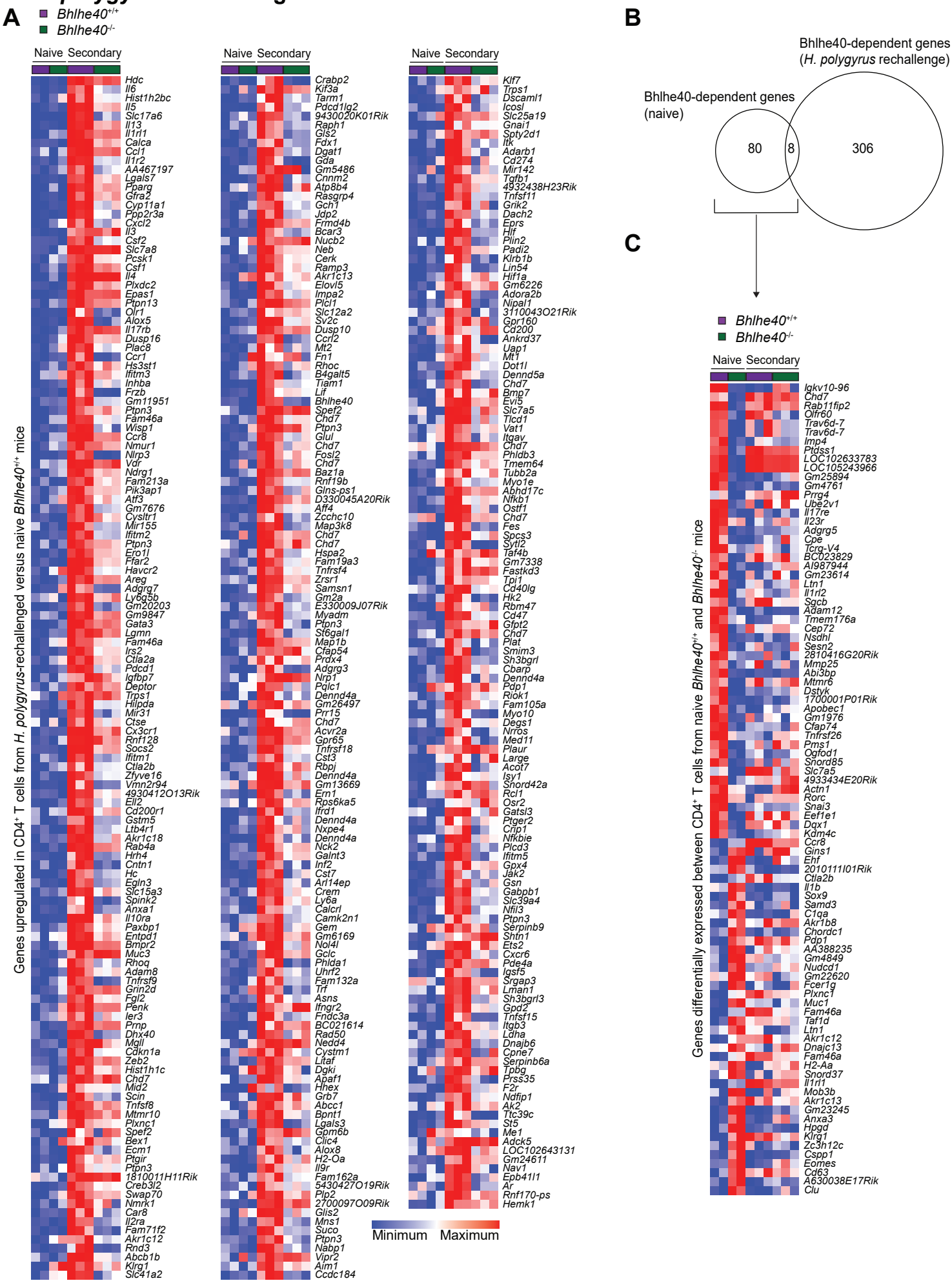

Figure S3: Bhlhe40 is required in T cells for normal cytokine production during *H. polygyrus* rechallenge

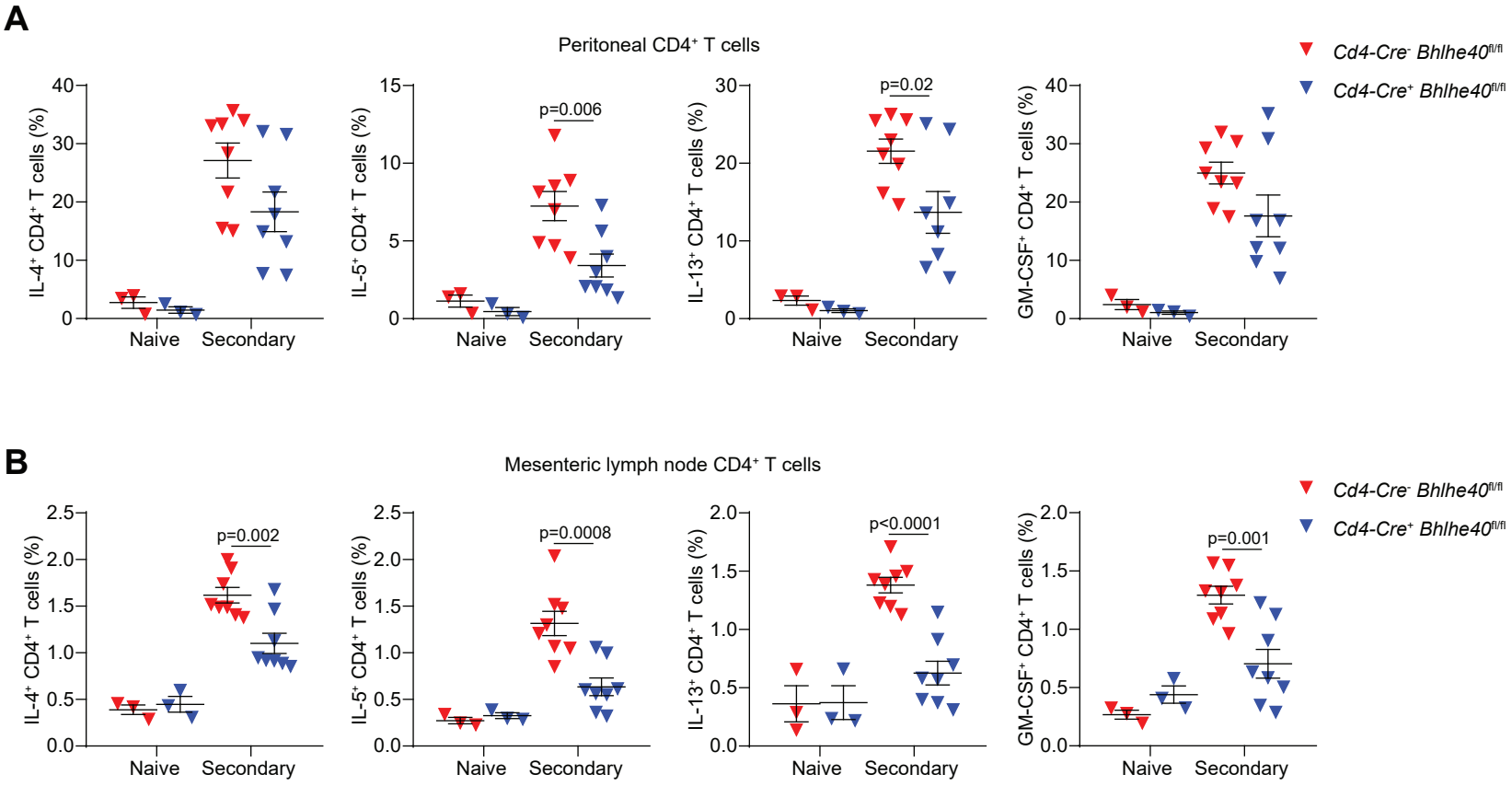
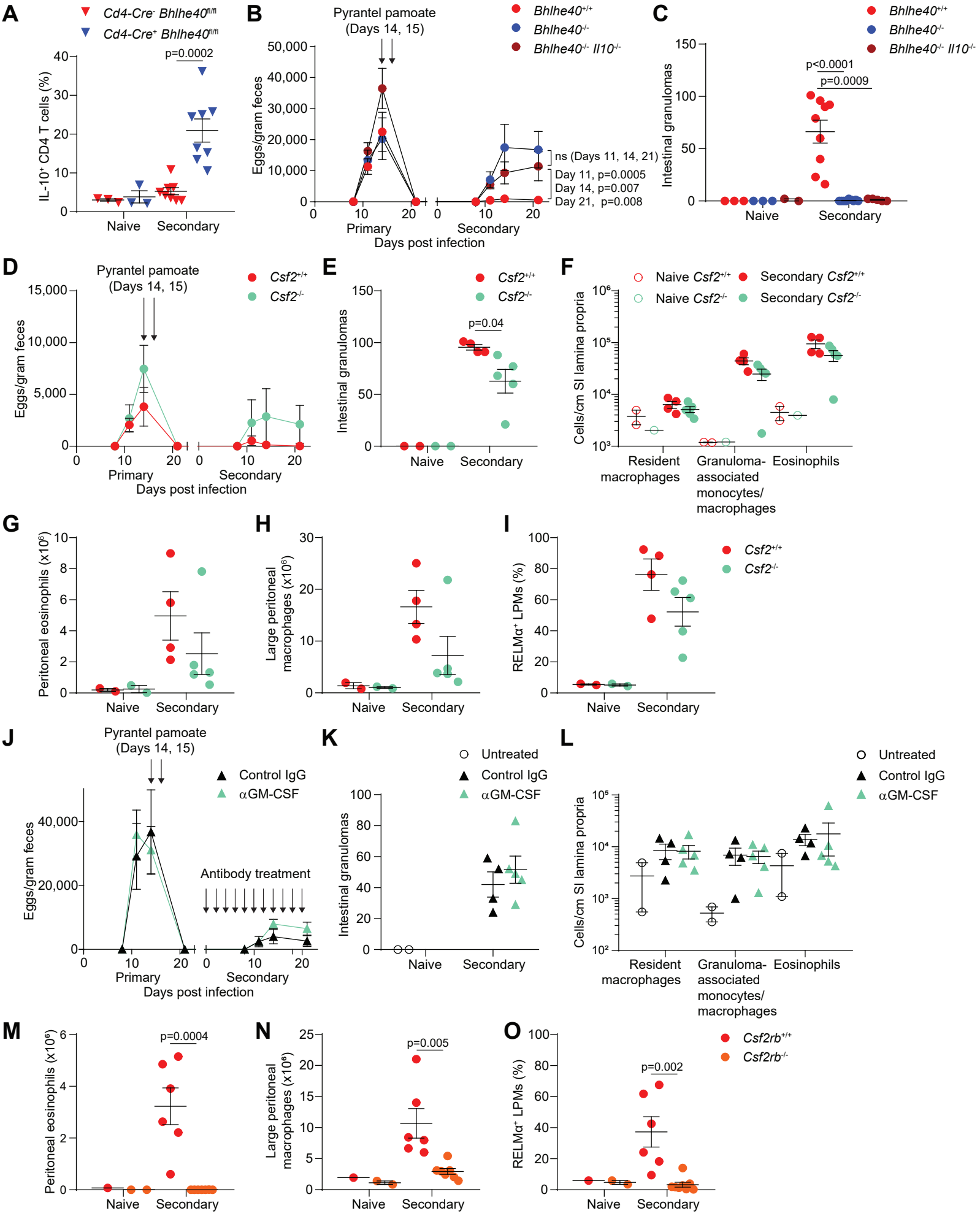
Figure S4: Further analysis of cytokine regulation during *H. polygyrus* rechallenge